NRL Report 6749

NRL Terrain Clutter Study Phase II

JOHN C. DALEY, WILLIE T. DAVIS, JAMES R. DUNCAN,
AND MICHAEL B. LAING

Wave Propagation Branch
Electronics Division

October 21, 1968

NAVAL RESEARCH LABORATORY
Washington, D.C.

This document has been approved for public release and sale; its distribution is unlimited.

The report on Phase I of this problem is NRL Report 6487, "NRL Terrain Clutter Study Phase I," N. W. Guinard, J. T. Ransone, Jr., M. B. Laing, and L. E. Hearton, May 10, 1967.

CONTENTS

Abstract	ii
Problem Status	ii
Authorization	ii
INTRODUCTION	1
INSTRUMENTATION	1
CLUTTER CROSS SECTION	3
TERRAIN DESCRIPTION	4
CLUTTER MAPS	9
TERRAIN CLUTTER DATA	10
POLARIZATION DEPENDENCE	21
WAVELENGTH DEPENDENCE OF TERRAIN CLUTTER	21
SYSTEMS LIMITATIONS	33
CONCLUSIONS	33
REFERENCES	35
APPENDIX A - Sample Clutter Map	36

ABSTRACT

The second and final phase of a terrain clutter study has been completed at Naval Research Laboratory utilizing the Four-Frequency Radar System installed in a WV-2 (Super Constellation) aircraft, BuNo 128324. This system is capable of transmitting and receiving four frequencies (P,X,L, and C) consecutively with a choice of horizontal, vertical, and alternating polarizations. The returns are gated at a fixed range and analyzed in a digital computer. Absolute clutter measurements have been taken over several sites at angles of incidence from 5 degrees to 60 degrees. The parameter measured was the normalized radar cross section in terms of the median value of its probability distribution. Data were obtained for this parameter as a function of incident angle, transmitted and received polarization, and radar wavelength for a wide variety of terrain types such as desert, mountainous, urban, and water. A significant conclusion was that the wavelength dependence of the terrain clutter varies from $n \approx 0$ for urban terrain to $n \approx 3/2$ for marshes.

PROBLEM STATUS

This is the final report on the final phase of the problem. Unless otherwise notified, this problem will be considered closed thirty days following the issuance of this report.

AUTHORIZATION

NRL Problem R07-02
AF MIPR AS-6-157

Manuscript submitted May 27, 1968.

NRL TERRAIN CLUTTER STUDY
PHASE II

INTRODUCTION

The Naval Research Laboratory has concluded a clutter measurement program for the Research and Technology Division, Systems Engineering Group, Wright-Patterson AFB, Ohio. The purpose of this work, as stated in the MIPR AS-5-64, is "to contribute technical data to establish clutter models... that can be used for theoretical evaluation of various rejection techniques...." The program has been divided into two phases. The initial phase concentrated upon the acquisition of clutter data at four frequencies and for both linear polarizations. These were taken at shallow angles of incidence (less than 10°) over both Canadian and American terrain. A report (1) describing the measurements and results of the Phase I program has been written and contains information not only on the instrumentation but also on the processing techniques used to derive the spectrum and radar cross section (RCS) of the clutter. Consequently, these details will largely be omitted in this report.

The emphasis of the second and final phase of the effort has been placed primarily upon the implementation of a specific clutter model (2) which required, as an input, maps of terrain scattering which consist of contiguous, equisized resolution cells. The RCS of each cell is specified in terms of its median value and cumulative probability distribution. In general, these are functions of the frequency, polarization, angle of incidence, and terrain type. The cross-section maps were constructed by digitally processing the range-gated returns of the Four-Frequency Radar (4FR) System in the NRL Research Computation Center CDC 3870 computer. A description of this study program will be given later in this report.

Since several independent samples of the RCS of the individual resolution cells are required to accurately compute the median RCS and distribution, the dwell time of the radar beam was increased by illuminating the terrain in a sidelooking, searchlight mode. In this mode, the antennas are fixed at right angles to the flight path and at a chosen elevation angle. The angles are held relatively constant by a stabilized antenna mount which is referenced to the vertical and magnetic north. The angle of incidence was varied by stepping the elevation angle as the aircraft made repeated runs at a fixed altitude, back and forth along a fixed flight path. The flight path was chosen to cross reasonably homogeneous terrain, i.e., not containing visible terrain boundaries.

Of the several flights made in 1966-1967, three were used to provide the majority of the data for both the clutter model and this report. These flights are listed in Table 1 together with the pertinent radar parameters and terrain descriptors. The data collected on these flights contain information of much greater scope than the definition of resolution cells; namely, the large-scale variation of the terrain clutter with the various radar parameters as well as with the terrain. Consequently, in addition to the details of implementing the clutter model, studies relating to the functional dependence of the RCS of various types of terrain on wavelength, polarization, and angle of incidence will be presented in the body of the report.

INSTRUMENTATION

A brief resume of the 4FR System will be given at this point to aid interpretation of the Phase II measurement program. The 4FR System is a research radar installed in an

Table 1
Flight Summary

Terrain	Frequency	Polarization	Elevation Angle, θ (deg)	PRF (pps)	Pulsewidth (μsec)
October 6, 1966					
Arizona desert	X band	VV,HH,VH,HV	5° → 50°	683	0.5
	C band	VV,HH,HV	5° → 50°	683	0.5
Arizona Mountainous terrain	X,L,P	VV,HH,VH,HV	8° → 50°	683	0.5
	C	VV,HH,HV	8° → 50°	683	0.5
October 7, 1966					
Arizona desert	L,P	VV,HH,VH,HV	8° → 50°	683	0.5
Phoenix and Suburbs	X,L,P	VV,HH,VH,HV	5° → 75°	683	0.5
	C	VV,HH,HV	5° → 75°		
Arizona eroded desert	X	VV,HH,VH,HV	5° → 12°	683	0.5
	C	VV,HH,HV	5° → 12°		
Arizona rough hills	X,L,P	VV,HH,VH,HV	8° only	683	0.5
	C	VV,HH,HV	8° only		
Arizona cultivated farmland	X,L,P	VV,HH,VH,HV	8° only	683	0.5
	C	VV,HH,HV	8° only	683	0.5
January 30, 1967					
New Jersey residential areas	X,L	VV,HH,VH,HV	8° → 60°	603	0.5
	C	VV,HH,HV	8° → 60°		
New Jersey rural	X,L	VV,HH,VH,HV	8° → 60°	603	0.5
	C	VV,HH,HV			
	P	VV,HH			
New Jersey Marshland	X,L	VV,HH,VH,HV	8° → 60°	603	0.5
	C	VV,HH,HV			
	P	VV,HH			
Delaware Bay 10-15 knot wind Whitecaps	X	VV,HH,VH	8° → 60°	603	0.5
	C	VV,HH	8° → 60°		
	L	VV,HH	8° → 60°		
	L	VH	8° → 12°		
	P	VV	8° → 60°		
	P	HH	12° → 60°		

EC-121 (Super Constellation) aircraft operated by a Navy crew. The instrumentation is operated and maintained as an NRL facility. The primary function of the 4FR System is to measure target characteristics at four different frequencies as well as for both linear polarizations. The system is capable of transmitting a pulse sequence of the form P_H, X_H, L_H, C_H, P_V, X_V, L_V, and C_V, where the band letters P, X, L, and C refer to the frequencies, 428 MHz, 8910 MHz, 1228 MHz, and 4455 MHz respectively, and the letters H and V refer to horizontally or vertically polarized transmissions. The pulse train has a variable repetition rate (100 to 2900 pps), and the width of the individual pulses is also variable (0.1 to 2 μsec). The antenna system, developed under Project Suspender, is mounted in the bottom radome of the EC-121 and is used for both transmission and reception. It consists of four dual polarized antennas. Two of these, which transmit X- and C-band energy, are mounted side by side and have collinear beams and equal beamwidths so that

they illuminate the same area. The L- and P-band antennas are mounted 180 degrees in azimuth away from the X- and C-band antennas and are likewise collinear. The beamwidths of these antennas are different so that the area illuminated by P-band energy includes the area illuminated by the L band. The antenna pairs, while locked in azimuth, are separately trained in elevation from 0° to 90°. The entire array may be scanned through 315° or any portion thereof.

Upon reception, the scattered return is separated into its orthogonal polarization components and amplified in parallel systems. The receivers in the 4FR System are time multiplexed in synchronism with the transmitted pulse burst to provide a more exact comparison between returns and also to simplify calibration. The components of the received signals are distinguished in this report by the addition of a second subscript to the transmitted form, i.e. X_{VH} refers to the horizontal return from a vertically polarized X-band transmission. All received signals are presented to an operator on an A-scope for gating. Regardless of the pulsewidth transmitted, a 30-nanosecond pulse is used to gate the return. After being gated, the phase and amplitude of the sample are digitized to seven-bit precision and recorded in the aircraft on magnetic tape for later processing. In all, 32 parameters the four amplitudes and all phases of the scattered components of four frequencies are recorded in each pass over the terrain at a rate corresponding to 32 times the repetition rate of the pulse burst.

CLUTTER CROSS SECTION

The radar cross section of a target, σ, is defined in the conventional way,

$$\sigma = \frac{(4\pi)^3 R^4 P_R}{\lambda^2 G^2 P_T} . \tag{1}$$

For an extended target, such as a patch of terrain, the normalized cross section, σ_0, is defined by

$$\sigma_0 = \frac{\sigma}{A} , \tag{2}$$

$$A \approx \frac{R\psi_a c\tau}{2\cos\psi} \quad \text{for small depression angles, and}$$

$$A \approx \frac{R^2\psi_a\theta_a}{\sin\psi} \quad \text{for large depression angles,}$$

where A is area illuminated by the radar, ψ_a and θ_a are the elevation and azimuthal beamwidths of the antenna, ψ is the angle of incidence, c is the speed of light, and τ is the pulse length.

Equation (2) assumes a uniform distribution of scatterers within the illuminated area. While this assumption is reasonably valid in the analysis of sea clutter, it is extremely difficult to find terrain that is sufficiently homogeneous to satisfy this definition. In particular, urban areas present strong divergences from homogeneous terrain due to the presence of large flat surfaces, which may be oriented perpendicular to the incident field. In spite of the difficulties, the normalized cross section will be used here because it does have the property of being normalized with respect to the area illuminated by the measurement radar.

The time sequence of the clutter amplitude at a fixed range is in general a nonstationary, nonhomogeneous, random process; consequently, the presentation of results offers special problems. In this measurement program, the data were processed to yield three different presentations. The first one was the maps referred to previously, which will be discussed in detail later. The second is a form introduced in the Phase I

report, the continuous plot of the 10%, 50% (median), and 90% level of successive cumulative probability distributions. These are the decibel values exceeded by 10%, 50%, and 90% of the signals in the sample. A fixed sample size, say 1000 pulses, is chosen, and the time history of the percentiles is recorded. The third form of presentation is the cumulative probability distribution of the entire run and is of value in determining large-scale RCS's and false-alarm rates of the given terrain. The ordinate of the distribution is the percentage of the sample size, while the abscissa is normalized cross section.

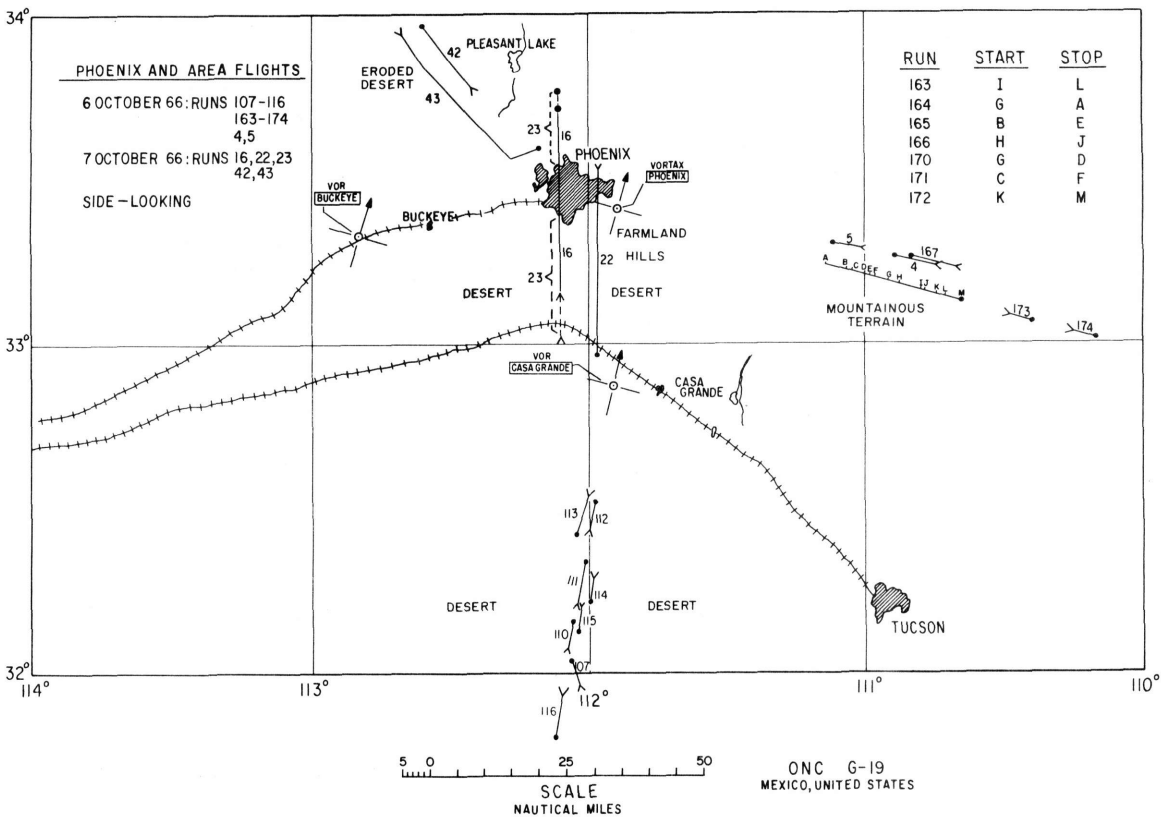

Fig. 1 - Phoenix, Arizona area

TERRAIN DESCRIPTION

In the Phase II Measurement Program, an attempt was made to provide terrain descriptions of the measured areas that are more exact than those of the Phase I program. One basic motivation was to attempt to correlate the gross features of the clutter maps with prominent terrain features. The specification of a given terrain in more quantitative terms is a formidable problem in itself and is beyond the desired scope of this report. Two means of identification were used. The first was an aircraft flight-path determination based upon VOR and the second, visual observations from the cockpit. From these, the maps shown in Figs. 1 and 2 were constructed. At several points on the map the terrain is described with various labels. These identify the terrain types which were chosen as homogeneous. For instance, Figs. 3 through 8 are photographs of terrains designated as desert, mountainous terrain, urban (Phoenix), eroded desert, rough hills, and cultivated farmland. In addition, data will be presented for which photographs are not available; namely, residential (Wildwood, N.J.), rural (New Jersey), marsh (New Jersey), and Delaware Bay. The latter is included in the measurement of the land-sea interface shown in Fig. 9. Figure 10 is the distribution of 26,000 samples taken for Run 16-X_{HH}. These are excellent illustrations of the processed data referred to in the previous section.

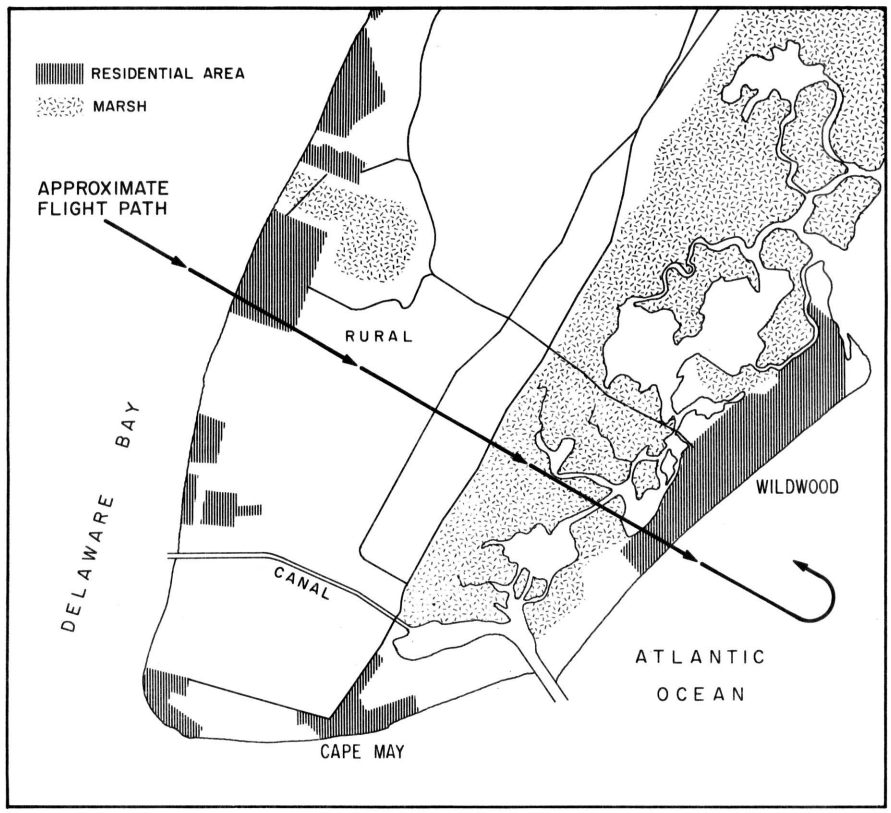

Fig. 2 - Cape May, New Jersey area

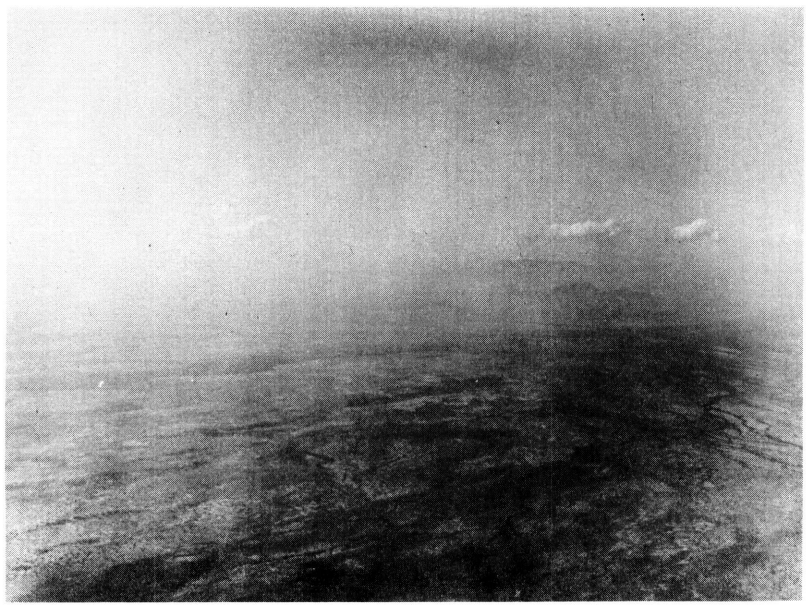

Fig. 3 - Arizona desert terrain

Fig. 4 - Arizona mountainous terrain

Fig. 5 - City of Phoenix

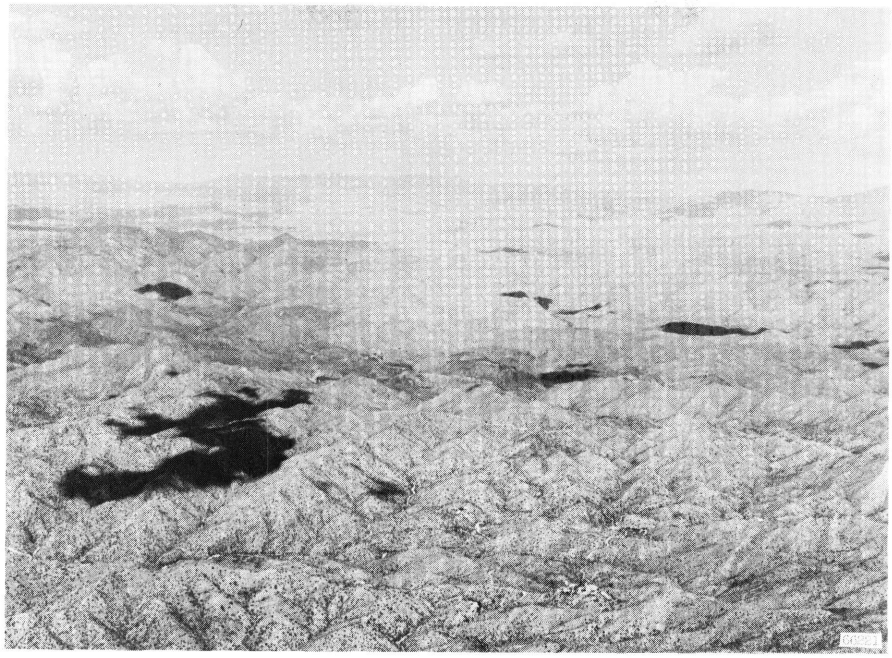

Fig. 6 - Eroded desert terrain

Fig. 7 - Hills south of Phoenix

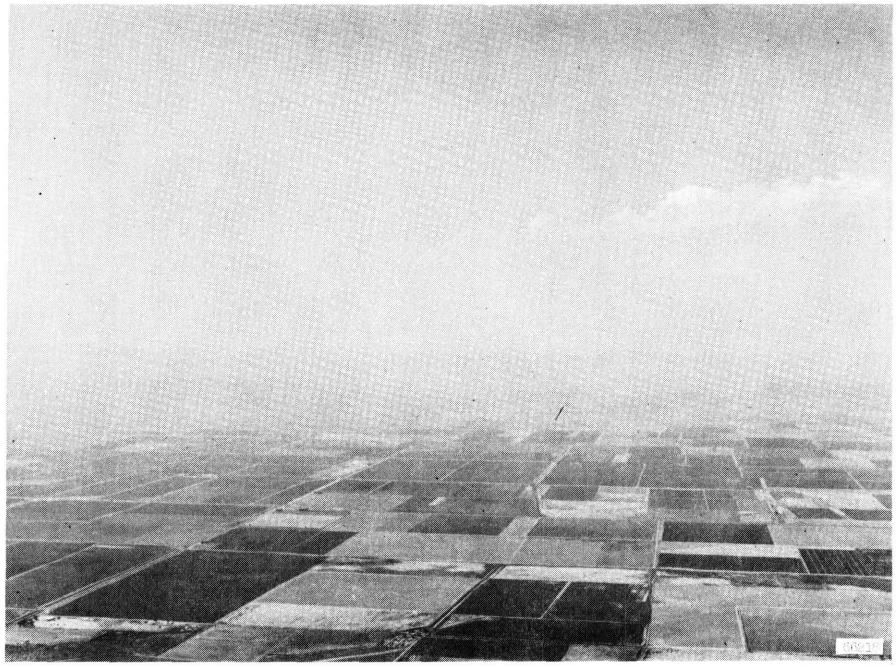

Fig. 8 - Cultivated farmland south of Phoenix

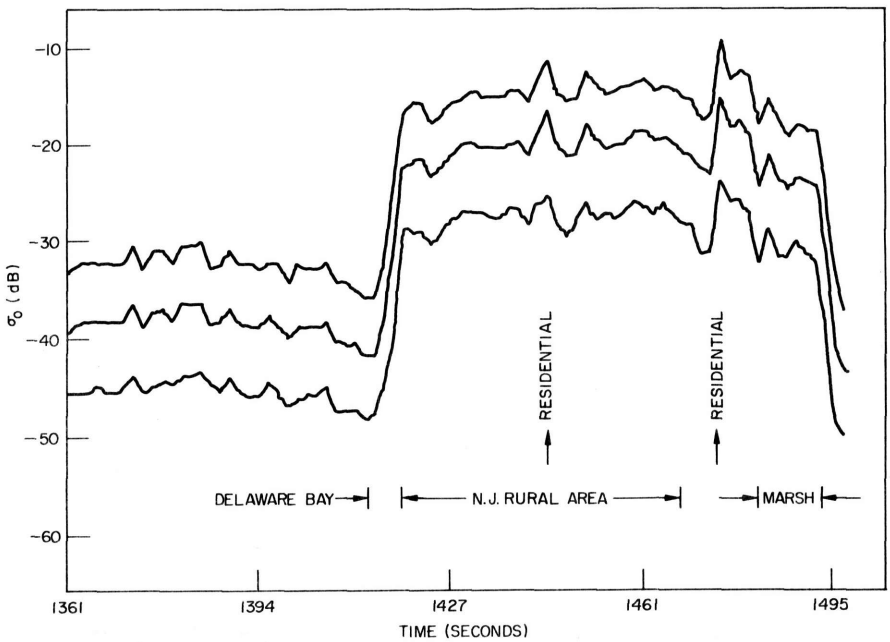

Fig. 9 - Sample cross section vs time plot, X_{HH}, $\theta = 8°$

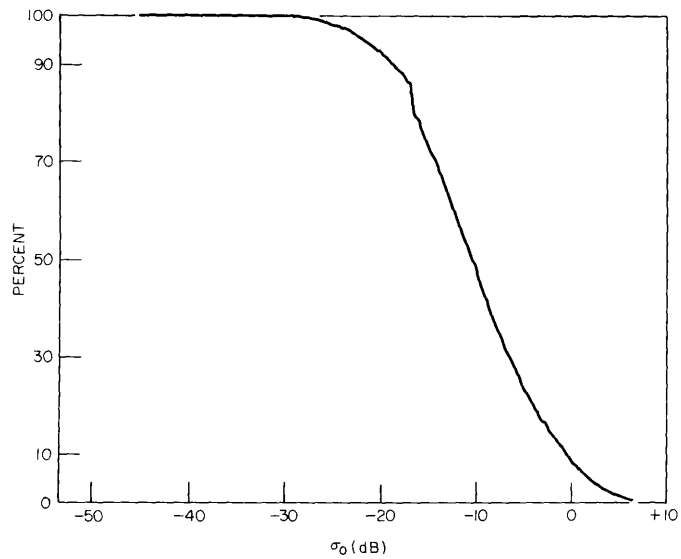

Fig. 10 - Cumulative probability distribution plot, X_{HH}, $\theta = 8°$

CLUTTER MAPS

The processing of data into resolution cells involves a knowledge of the flight parameters, such as speed and altitude, as well as the beamwidth. With these, the number of samples available to specify the statistical variation of a resolution cell is

$$K' = \frac{R f_r \theta_a \cos \psi}{2v} , \tag{3}$$

where f_r is the pulse repetition rate of the radar. To eliminate doppler fluctuations in the data, a smoothing window of length

$$T = \frac{L}{2v} \tag{4}$$

was used, where L is the length of the aperture in the azimuthal direction. This involved averaging every $N = T f_r$ pulses together so that the number of independent samples becomes

$$K = \frac{R \theta_a \cos \psi}{L} . \tag{5}$$

The resulting K pulses were distributed to determine the percentile values. This operation was repeated for each contiguous group of K' pulses to yield the clutter map. Appendix A consists of the map determined for Run 110, desert terrain, as well as the data required to calibrate the percentile values. It should be noted in the appendix that the zeroth percentile refers to the highest value of cross section observed in the sample.

Clutter maps (3) for the runs shown in Fig. 1, as well as data from Goose Bay, Labrador not shown in this report, were transmitted to analysts at the Illinois Institute of Technology Research Institute, Chicago, Illinois, to provide an input to their clutter model. Results of their analyses have been published (4) as well as their preliminary conclusions. The remainder of this report will deal with large-scale variations which are a continuation of the studies pursued in Phase I.

TERRAIN CLUTTER DATA

Some of the most useful data to the system designer is the variation of the median, normalized, cross section with incidence angle for a specified terrain. The data acquired in the Phase II program have been processed to yield this variation for each of the terrains measured. The basic data run, i.e., one similar to Fig. 9, was acquired in the side-looking mode previously described. The X- and C-band antenna systems were oriented at 90°, while the L- and P-band antennas were at 270°, with respect to the flight path. The signals returned from the portions of the flight path over the specified terrain were averaged to determine the value of normalized cross section that corresponds to the preset angle of incidence. The rural area in Fig. 9 was averaged to yield -20 decibels (dB) of normalized cross section.

To determine the variation with angle of incidence, the elevation angles of the beams were changed and the flight path reflown. The data presented in Fig. 11 show the resulting variation of normalized cross section with angle of incidence for each of the measured terrain types. Each of these figures is labeled with the frequency and transmit/receive polarization subscripts which characterize the echo. Figure 12 is similar, with the difference that these represent cross-polarized data obtained over the various terrains. Because of the stringent requirements for isolation between antennas, correct illumination, and minimum crosstalk in the sampling system, cross-polarization data is often erroneous; consequently, there are missing components in these figures. The sample sizes involved in these averages are extremely large, consisting in general of 10,000 to 20,000 data points which represent approximately 15 to 30 seconds of flying time or 1 to 2 miles of ground track. The urban data is an exception that will require further discussion.

Past experiments (5) have indicated that the normalized cross section is a slowly increasing function of the angle of incidence, which may be approximated by the sine function. This is borne out by the variation of the cross section of the rural, desert, and mountainous terrain in the figures. The exception to this trend is found in the urban data. This result is not unexpected in view of the nonhomogeneous nature of the terrain. The peaks shown at 8° angle of incidence may be explained by the specular reflection from buildings that occurs at this angle. In view of the great pulse-to-pulse fluctuations present in the urban data, a further analysis in terms of sample size is given in Fig. 13. In these, the maximum median value of cross section is plotted versus angle of incidence for two different sample sizes. Short sample-size (1000 data points) maxima are plotted as dashed lines in these figures. Figure 13 illustrates this analysis; the dashed curves are from samples located primarily in the center of Phoenix (see Fig. 5). The short sample represents 1.5 seconds of flight or approximately 450 ft along the ground track. The solid curves consist of large sample sizes (26,000 to 37,000 data points) so that these curves represent the variation of cross section with angle over large areas since they represent averages of data acquired in 38 to 54 seconds of flight time or over 2 to 3 miles along the ground track. Therefore, the larger samples include a smaller density of point targets than do the smaller ones.

The magnitude of the fluctuation in the urban data may be determined from the figures by comparing the respective values for a given plot. The difference between these can be seen to be as great as 15 dB, so that the nonhomogeneity of the terrain introduces a major consideration into the use of the cross section. The cross-section curves used in Figs. 11 and 12 for both the Phoenix and New Jersey urban areas use the shorter sample sizes, i.e., medians of 1000 data points.

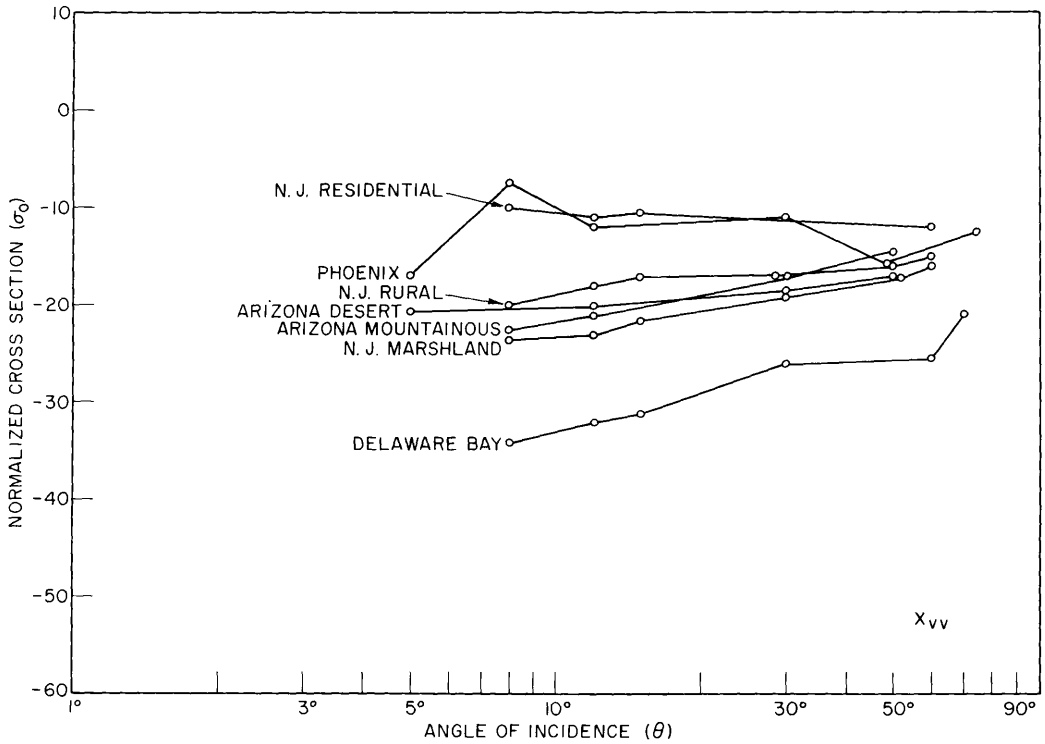

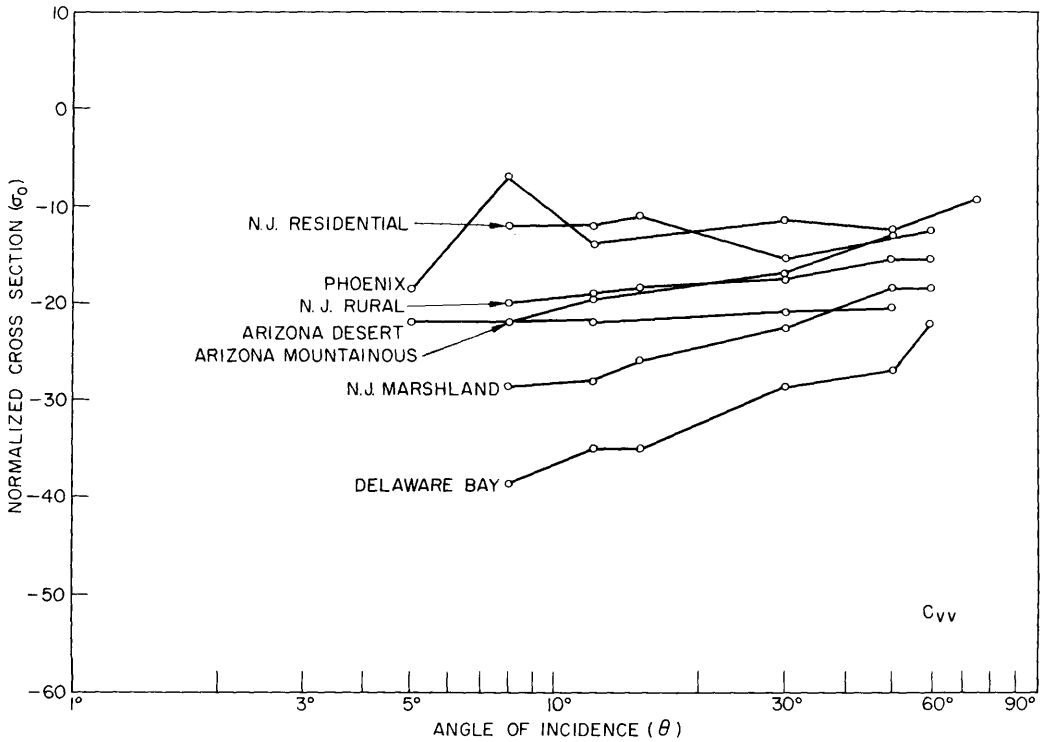

Fig. 11 - Variation of normalized cross section with incident angle (direct polarization)

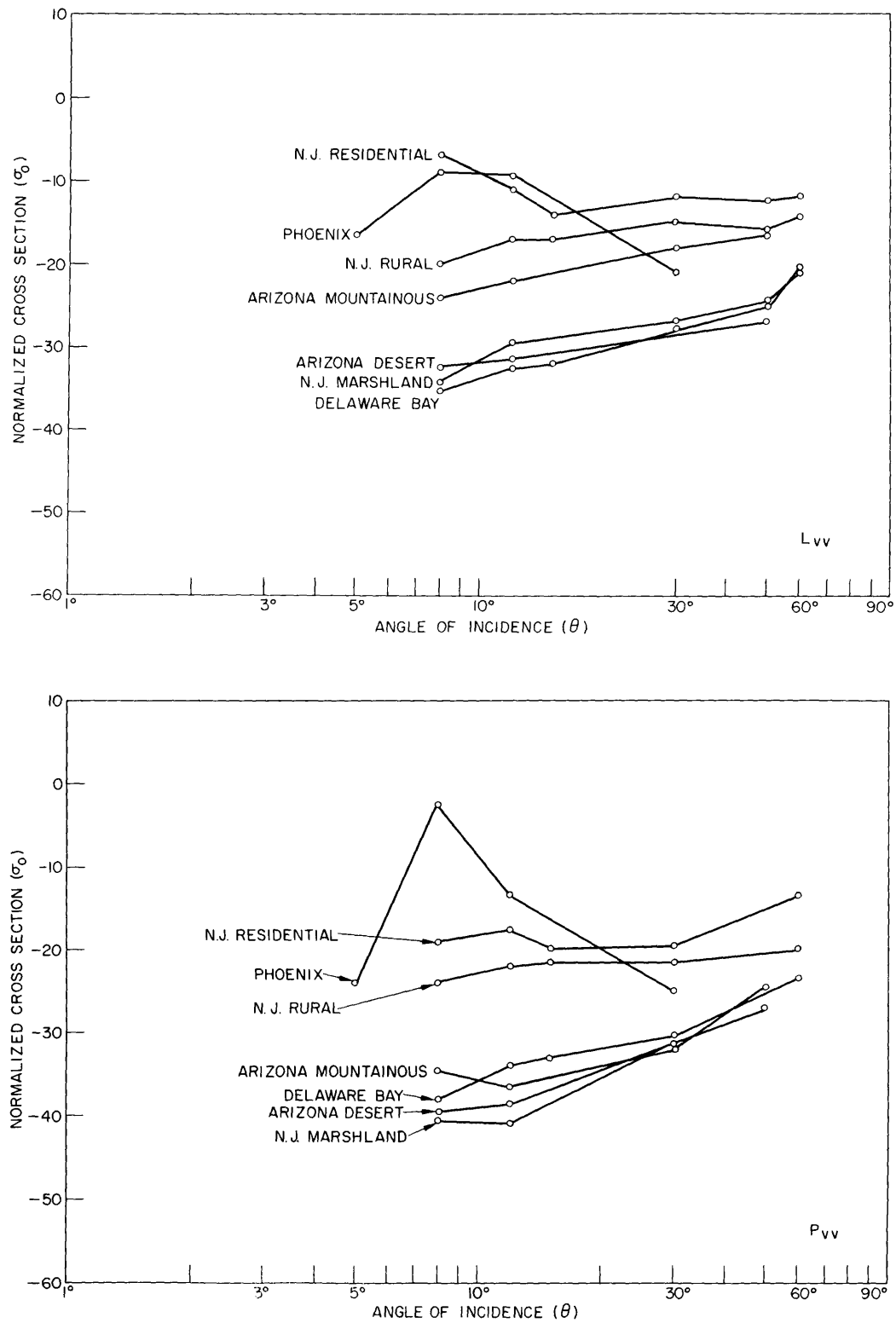

Fig. 11 (Continued) - Variation of normalized cross section with incident angle (direct polarization)

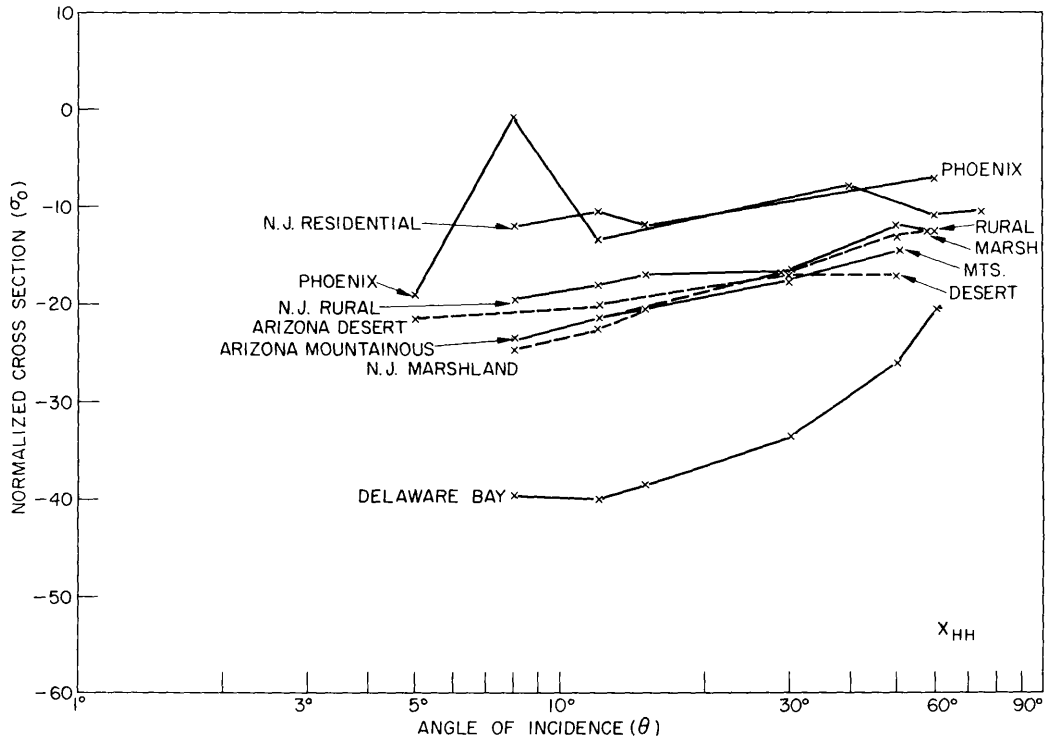

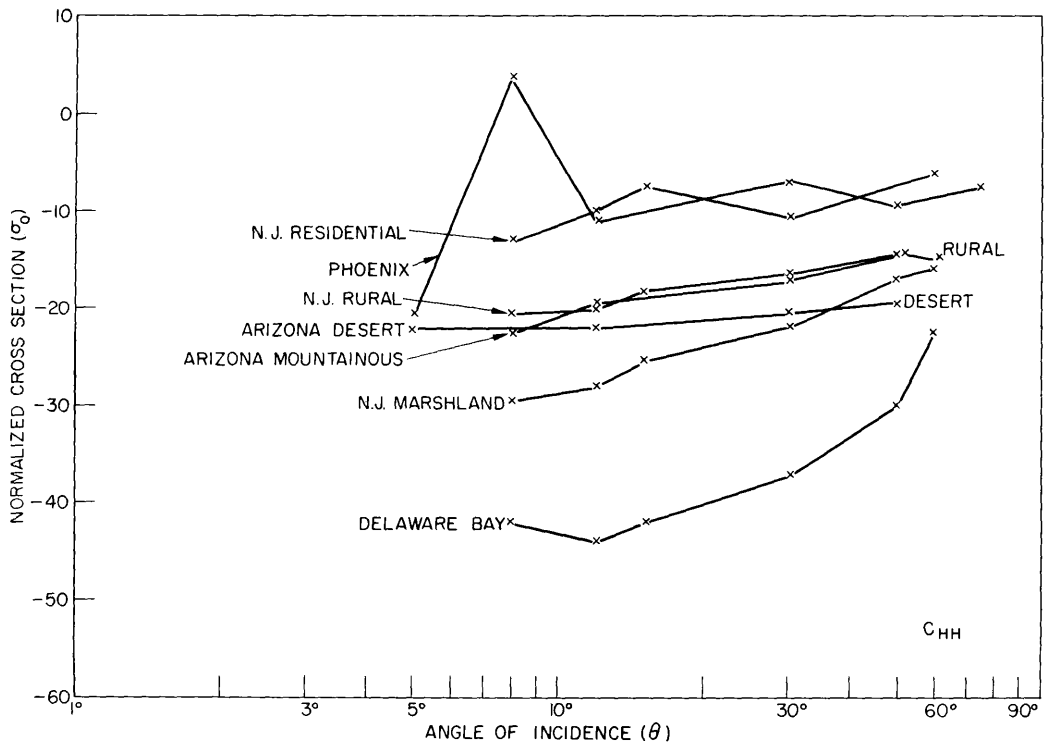

Fig. 11 (Continued) - Variation of normalized cross section with incident angle (direct polarization)

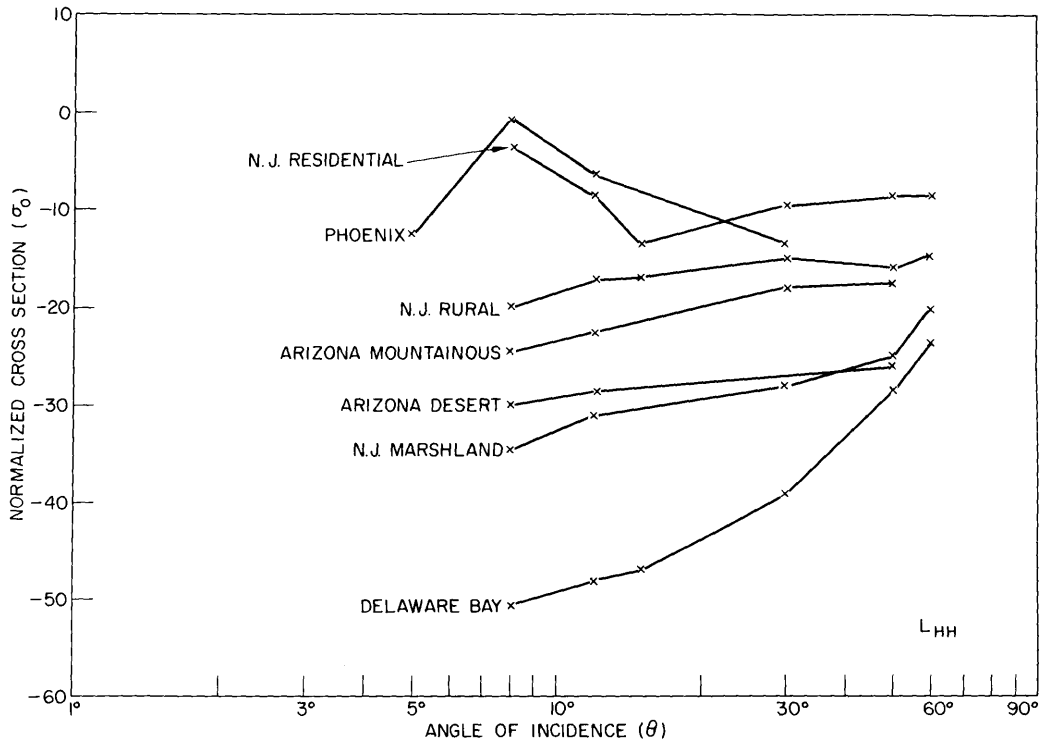

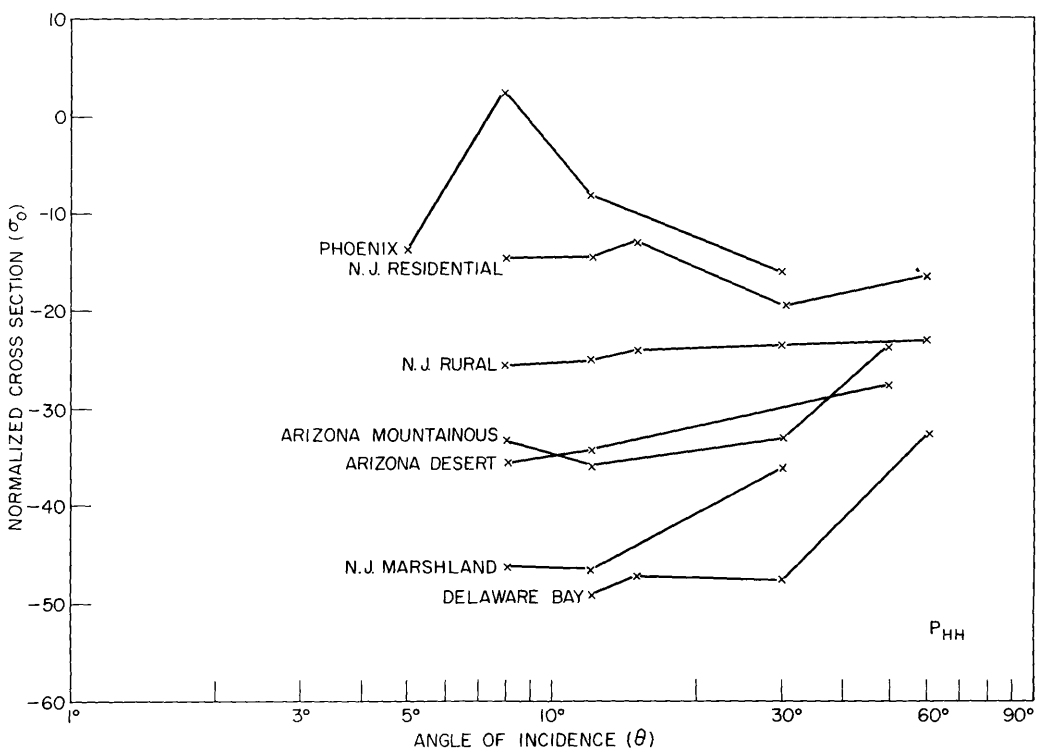

Fig. 11 (Continued) - Variation of normalized cross section with incident angle (direct polarization)

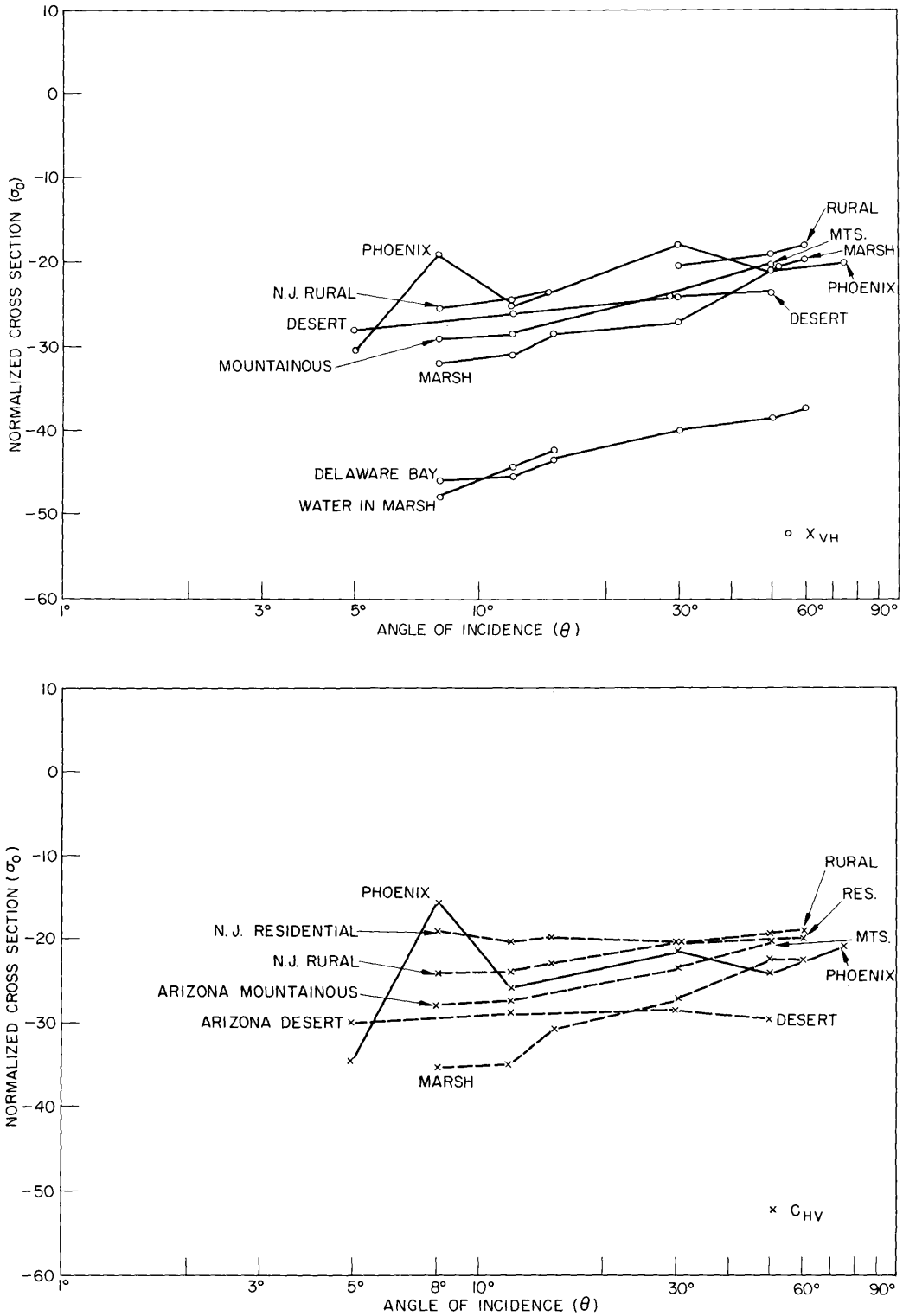

Fig. 12 - Variation of normalized cross section with incident angle (cross polarization)

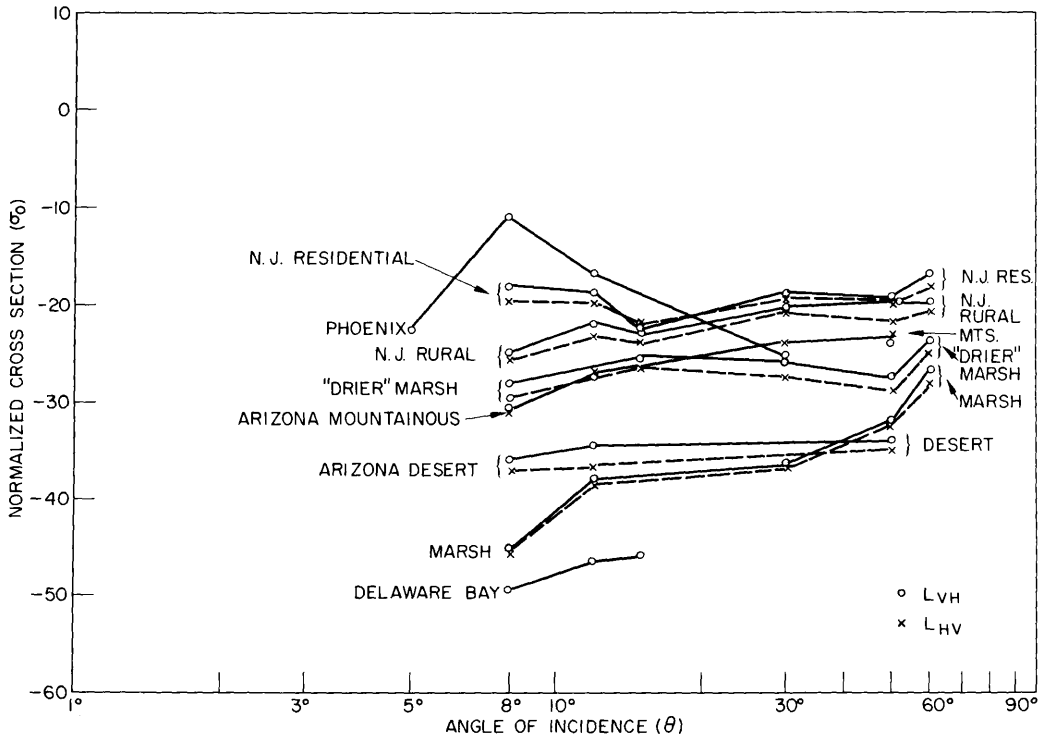

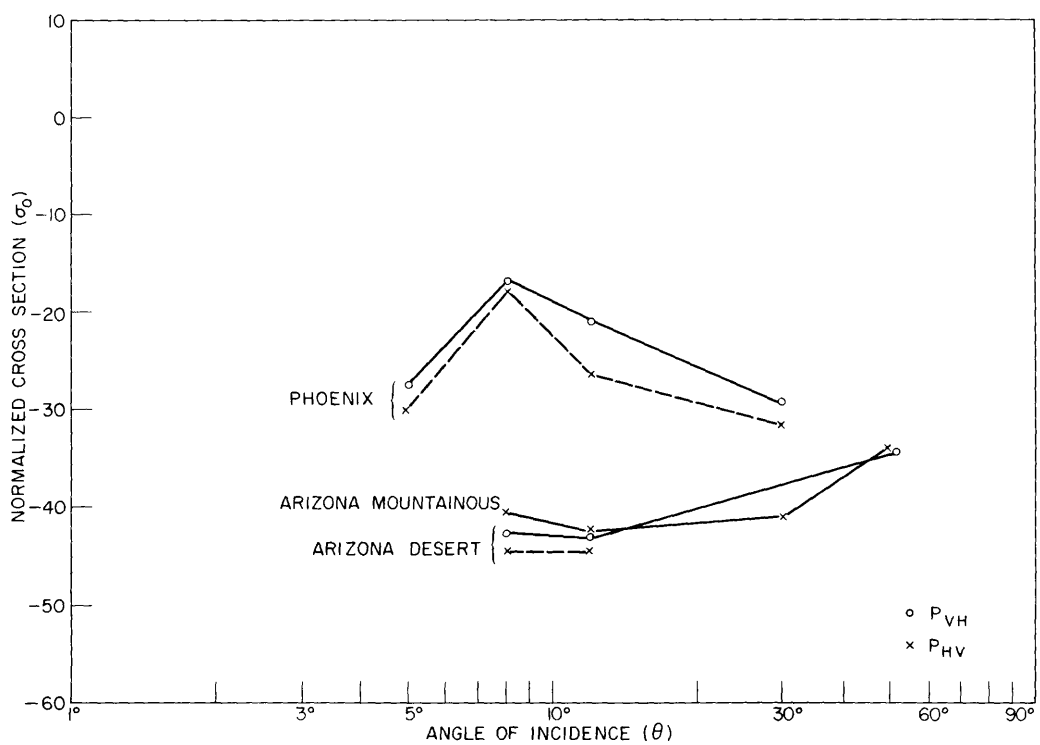

Fig. 12 (Continued) - Variation of normalized cross section with incident angle (cross polarization)

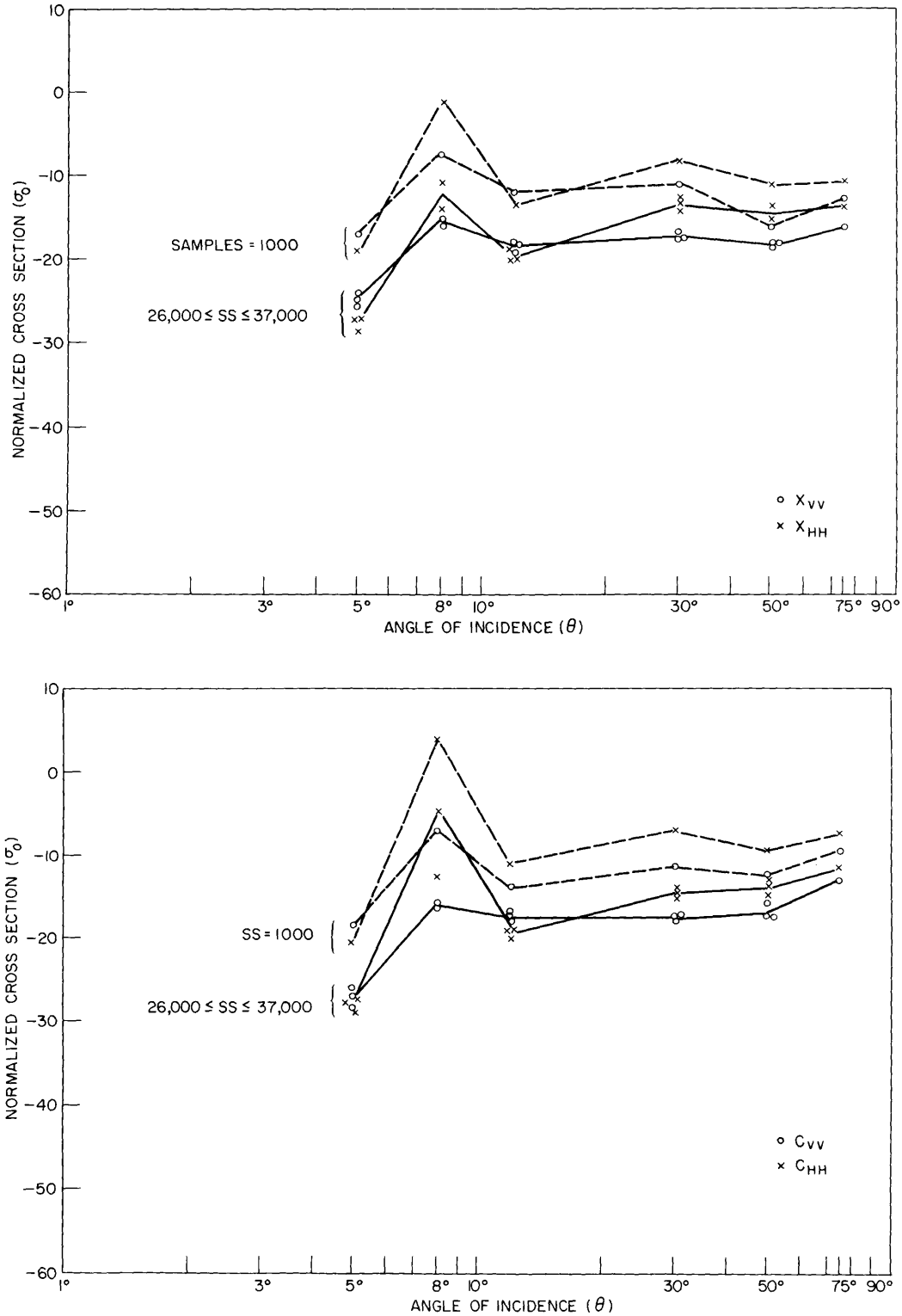

Fig. 13 - Variation of normalized cross section with incident angle, city of Phoenix

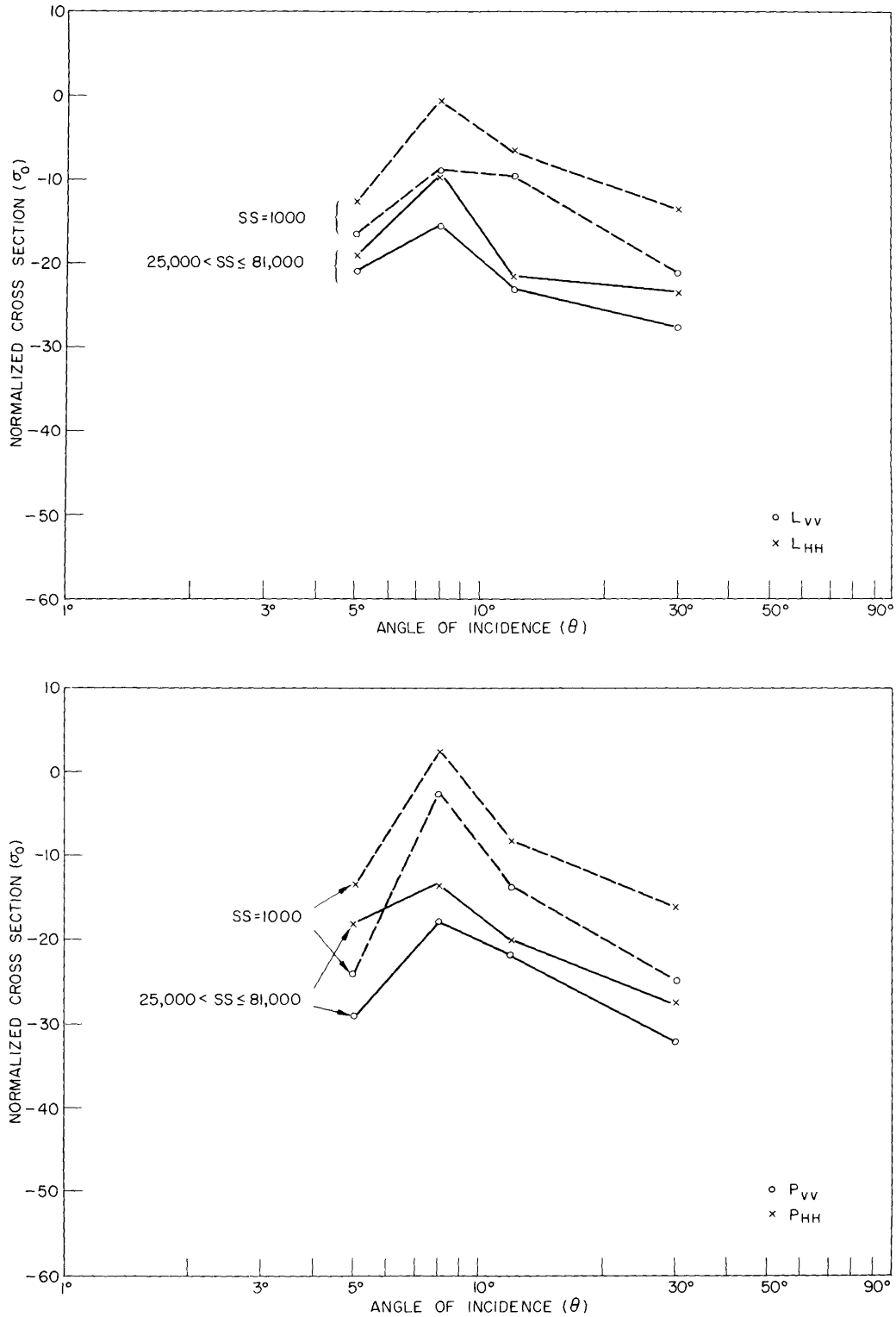

Fig. 13 (Continued) - Variation of normalized cross section with incident angle, city of Phoenix

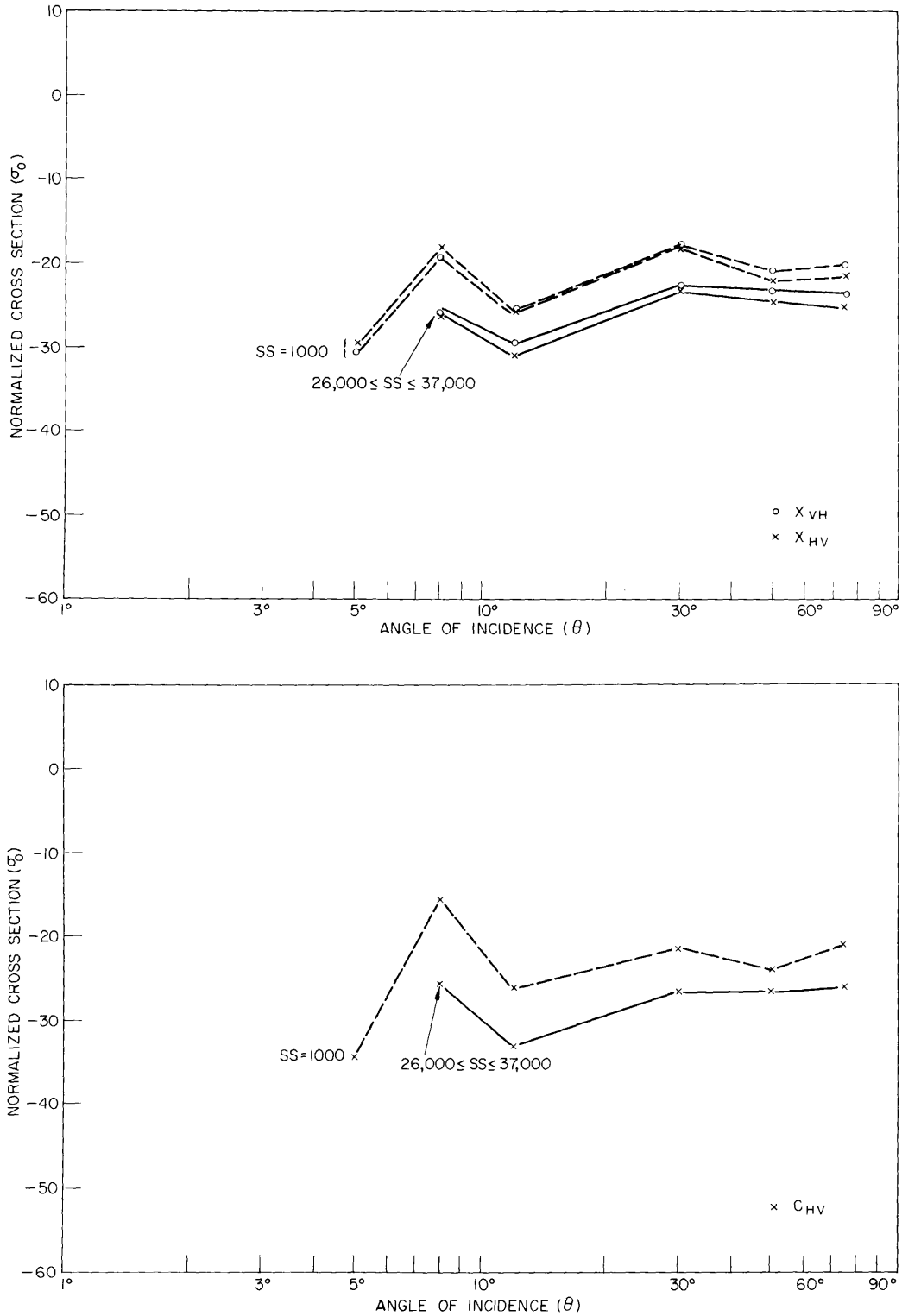

Fig. 13 (Continued) - Variation of normalized cross section with incident angle, city of Phoenix

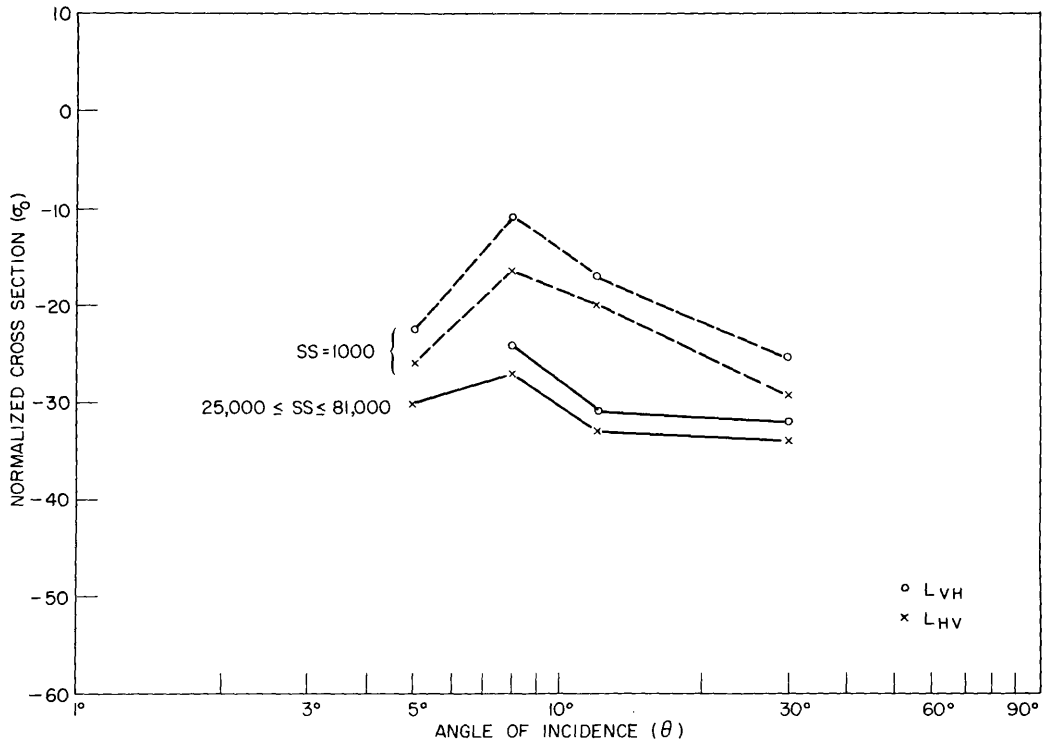

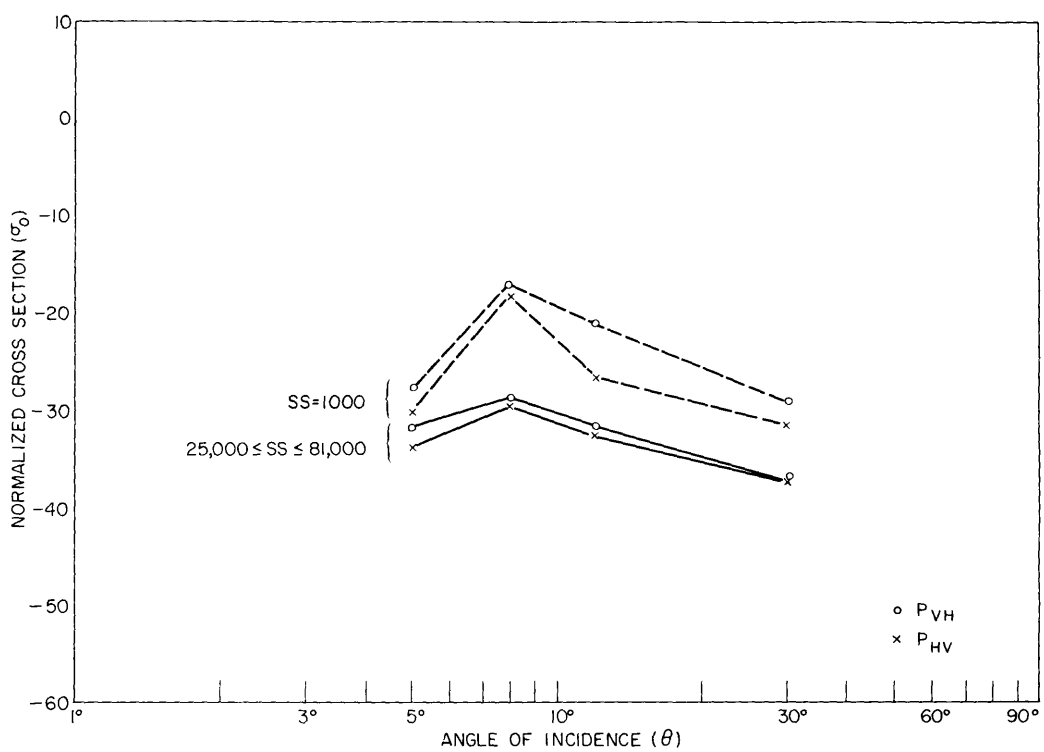

Fig. 13 (Continued) - Variation of normalized cross section with incident angle, city of Phoenix

POLARIZATION DEPENDENCE

The polarization dependence of cross section has been observed most strongly at shallow angles of incidence in relatively calm seas. Under these conditions, the ratio of the vertically polarized component to the horizontal, i.e., $\sigma_0(VV)/\sigma_0(HH)$ (the difference in dB) has been measured and found to be in the range of 10 to 1000. Equally strong ratios have been found in the cross section of certain man-made targets. Figure 14 gives plots of this ratio for the various frequencies and terrain types. As expected, Delaware Bay gives a large positive ratio, while other terrains tend to scatter about unity or slightly less. The mountainous and rural terrain have a small polarization ratio which is independent of wavelength. This is not so of the other terrains. For the bay and the marsh, the ratio decreases with increasing wavelength (Fig. 15). On the other hand, in the returns from the desert and the city of Phoenix, the direct polarization ratio increases with decreasing wavelength, although the variation is slight for the desert data. As occurred in the previous data, the urban return has the lowest polarization ratio and the highest horizontal direct return.

The cross-polarization characteristics of the scattering phenomenon may be examined by determining the cross-polarization ratio, σ_0 (VV)/σ_0 (HV). Values of this ratio are tabulated in Table 2 for the various terrain types investigated. The cross-polarization ratio for mountainous, desert, and rural returns shows no dependence on angle of incidence, while the marsh and residential areas of New Jersey have a decreasing polarization ratio with increasing angle. Table 3 gives a further analysis of this data. The nonhomogeneous terrains (urban Phoenix and New Jersey residential) have the largest cross-polarization ratios. Referring to previous figures show that while the vertically polarized direct return is large for these returns, the cross-polarized components are comparable to those of the more homogeneous terrains. This would seem indicative of specular reflection from flat surfaces, say, roofs and the sides of buildings. In addition, Fig. 13 shows that the cross-polarized components from the Phoenix terrain have less fluctuation than the corresponding directly polarized components.

WAVELENGTH DEPENDENCE OF TERRAIN CLUTTER

The data gathered to date indicate that the normalized cross section is, in general, a function of wavelength. This relation can be symbolized as

$$\sigma_0 \propto \lambda^{-n} . \tag{6}$$

The graphs of this variation for the various terrains are given in Fig. 16 for the direct and cross polarized returns beginning with an elevation angle of 8°. For the urban Phoenix and residential New Jersey data, the value of n is approximately zero. That is reasonable since the large fluctuations present in the data would tend to obliterate any slow variations such as $n \approx 1$ which have been observed for more homogeneous terrains. The rural and mountainous terrain show $n \approx 0$ from X-band to L-band; however, P-band is considerably lower in the mountainous terrain. The rough hills, desert, and cultivated farmland repeat a result obtained in the previous measurement program; namely, a wavelength dependence with $n \approx 1$. Marsh data on the other hand show a stronger dependence, $n \approx 3/2$. The above trends describe both direct and cross polarization. A repetition of the data with the incidence angle changed to 30° (Fig. 16) indicates little change in the wavelength dependence for the various terrains. Consequently, the data presented indicate that the wavelength dependence of terrain clutter is independent of polarization of the incident signal and also of the angle of incidence (Fig. 17).

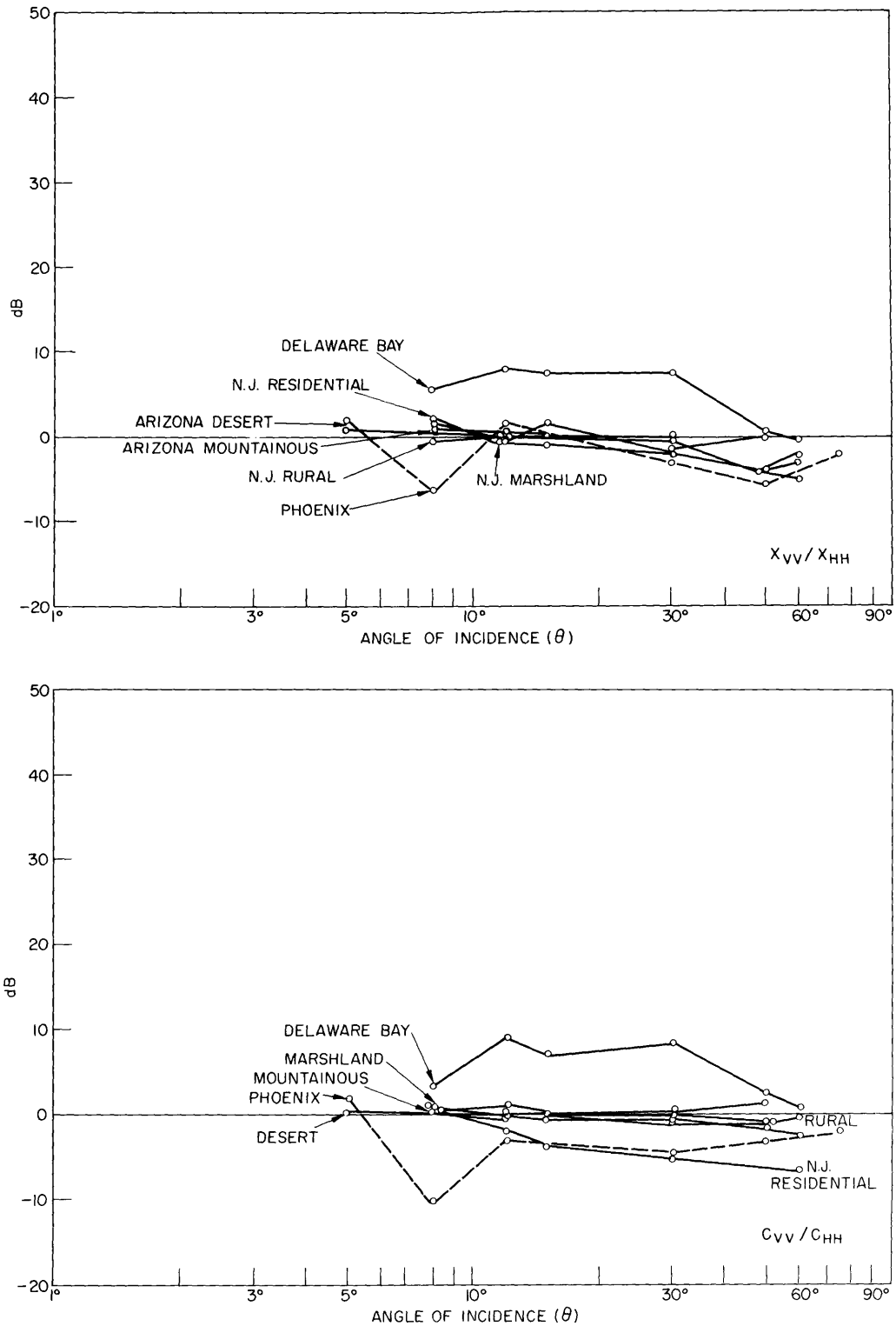

Fig. 14 - Direct polarization ratio vs incident angle

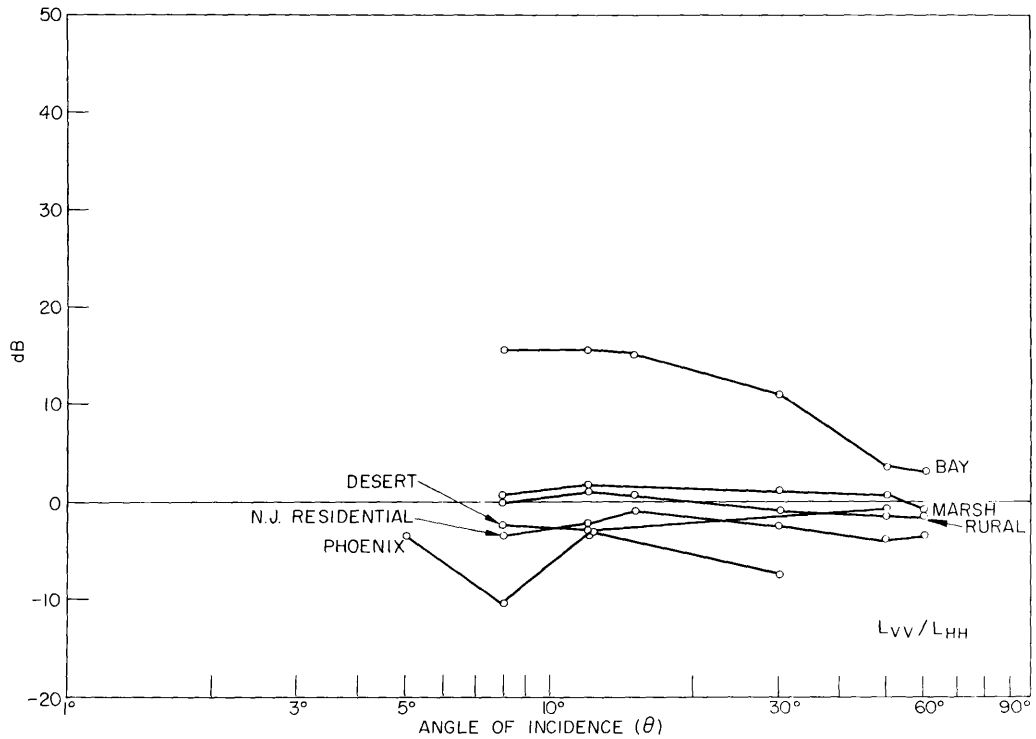

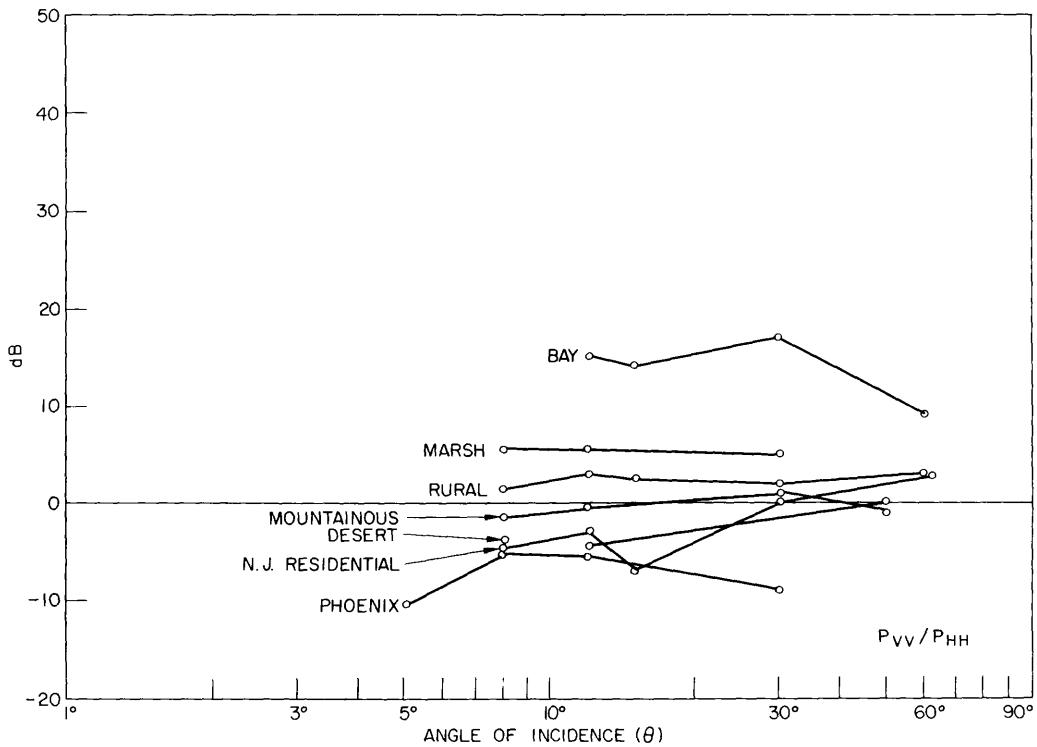

Fig. 14 (Continued) - Direct of polarization ratio vs incident angle

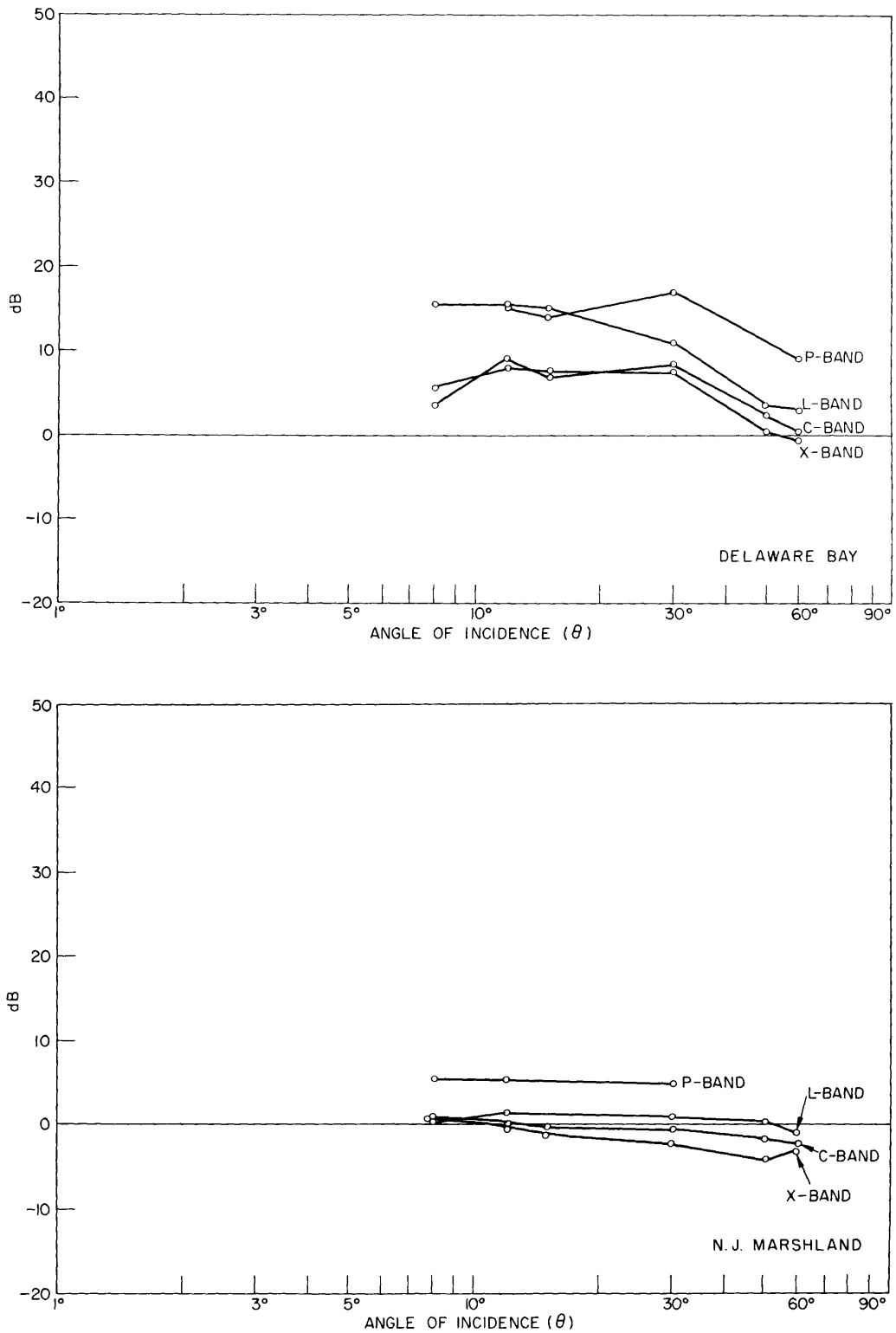

Fig. 15 - Direct polarization ratio vs wavelength

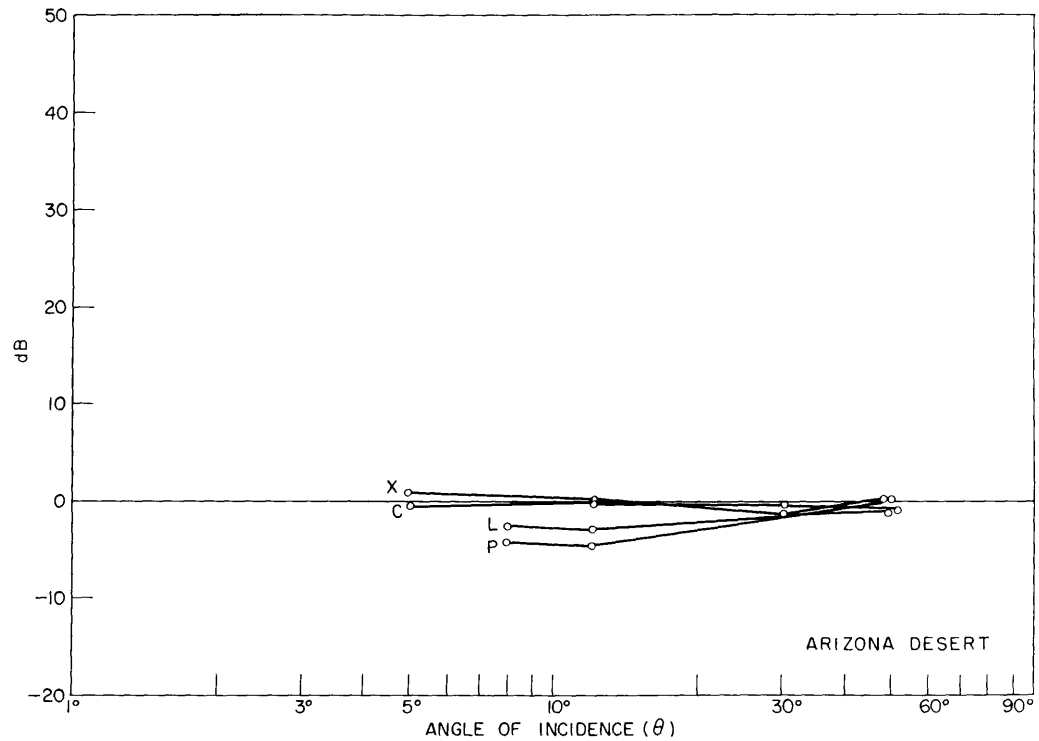

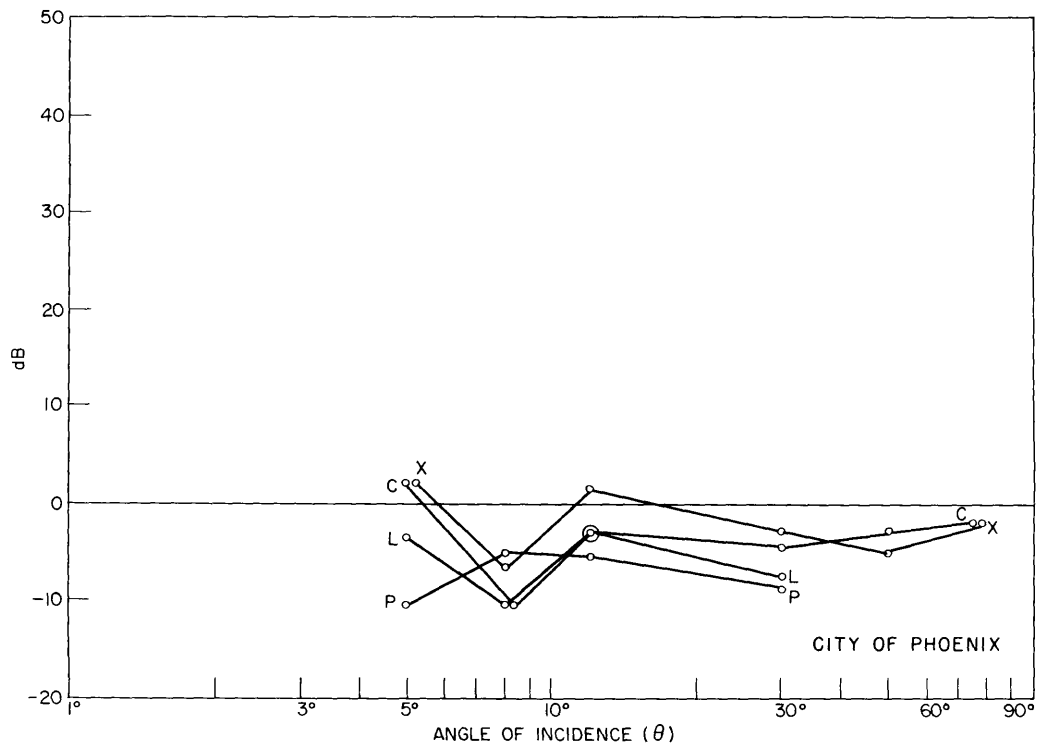

Fig. 15 (Continued) - Direct polarization ratio vs wavelength

Table 2
Cross-Polarization Ratios
σ_0(VV)/σ_0 (HV)

θ	X VV/HV	C VV/HV	L VV/HV	P VV/HV
Desert				
5°	+ 7-1/2	+ 8	-	-
8°	-	-	+ 4-1/2	+ 4-1/2
12°	+ 6	+ 7	+ 5-1/2	+ 6
30°	+ 6	+ 7-1/2	-	-
50°	+ 7-1/2	+ 9	+ 7-1/2	-
60°	-	-	-	-
75°	-	-	-	-
Marsh				
5°	-	-	-	-
8°	+ 9-1/2	+ 7	+11-1/2	None
12°	+ 7-1/2	+ 7	+ 9	None
15°	+ 6-1/2	+ 5	-	None
30°	+ 6-1/2	+ 5	+10	None
50°	+ 5	+ 4	+ 7-1/2	None
60°	+ 4-1/2	+ 4	+ 7-1/2	None
75°	-	-	-	-
Phoenix; SS > 25,000				
5°	-	-	+ 9	+ 2-1/2
8°	+10-1/2	+ 9-1/2	+11-1/2	+10-1/2
12°	+13	+15-1/2	+10	+10-1/2
15°	-	-	-	-
30°	+ 6	+ 9	+ 6-1/2	+ 5
50°	+ 6-1/2	+ 9-1/2	-	-
60°	-	-	-	-
75°	+ 9	+13	-	-
New Jersey Residential				
8°	+12-1/2	+ 7	+12-1/2	None
12°	+11	+ 8-1/2	+ 9	None
15°	+ 9	+ 9	+ 8	None
30°	+10-1/2	+ 5	+ 7-1/2	None
50°	-	-	+ 7-1/2	None
60°	+ 8-1/2	+ 7-1/2	+ 6-1/2	None
Mountains				
5°	-	-	-	-
8°	+ 6	+ 5-1/2	+ 7	+ 5
12°	+ 6-1/2	+ 8	+ 5	+ 6
30°	+ 6	+ 6	+ 6	+ 9
50°	+ 6	+ 6	+ 5-1/2	+ 9-1/2
60°	-	-	-	-
75°	-	-	-	-
Phoenix; SS = 1000				
5°	+12-1/2	+16	+ 9-1/2	+ 6
8°	+11-1/2	+ 8-1/2	+ 7-1/2	+15-1/2
12°	+13-1/2	+12	+10-1/2	+13
15°	-	-	-	-
30°	+ 7	+10	+ 8-1/2	+ 6-1/2
50°	+ 6	+11-1/2	-	-
60°	-	-	-	-
75°	+ 9	+11-1/2	-	-
New Jersey Rural				
5°	-	-	-	-
8°	+ 7	+ 4	+ 5-1/2	None
12°	+ 7	+ 5	+ 6-1/2	None
15°	+ 8	+ 4-1/2	+ 7	None
30°	+ 4	+ 3	+ 6	None
50°	+ 4-1/2	+ 4	+ 6	None
60°	+ 5	+ 3-1/2	+ 6-1/2	None
75°	-	-	-	-

Table 3
Cross-Polarization Ratios

Terrain	X VV/HV	C VV/HV	L VV/HV	P VV/HV
θ = 12°				
Marsh	+ 7-1/2	+ 7	+ 9	-
Desert	+ 6	+ 7	+ 5-1/2	+ 6
Mountains	+ 6-1/2	+ 8	+ 5	+ 6
New Jersey rural	+ 7	+ 5	+ 6-1/2	-
Phoenix; SS > 25,000	+13	+15-1/2	+10	+10-1/2
New Jersey residential	+11	+ 8-1/2	+ 9	-
Phoenix; SS = 1000	+13-1/2	+12	+10-1/2	+13
θ = 30°				
Marsh	+ 6-1/2	+ 5	+10	-
Desert	+ 6	+ 7-1/2	-	-
Mountains	+ 6	+ 6	+ 6	+ 9
New Jersey rural	+ 4	+ 3	+ 6	-
Phoenix; SS > 25,000	+ 6	+ 9	+ 6-1/2	+ 5
New Jersey residential	+10-1/2	+ 5	+ 7-1/2	-
Phoenix; SS = 1000	+ 7	+10	+ 8-1/2	+ 6-1/2

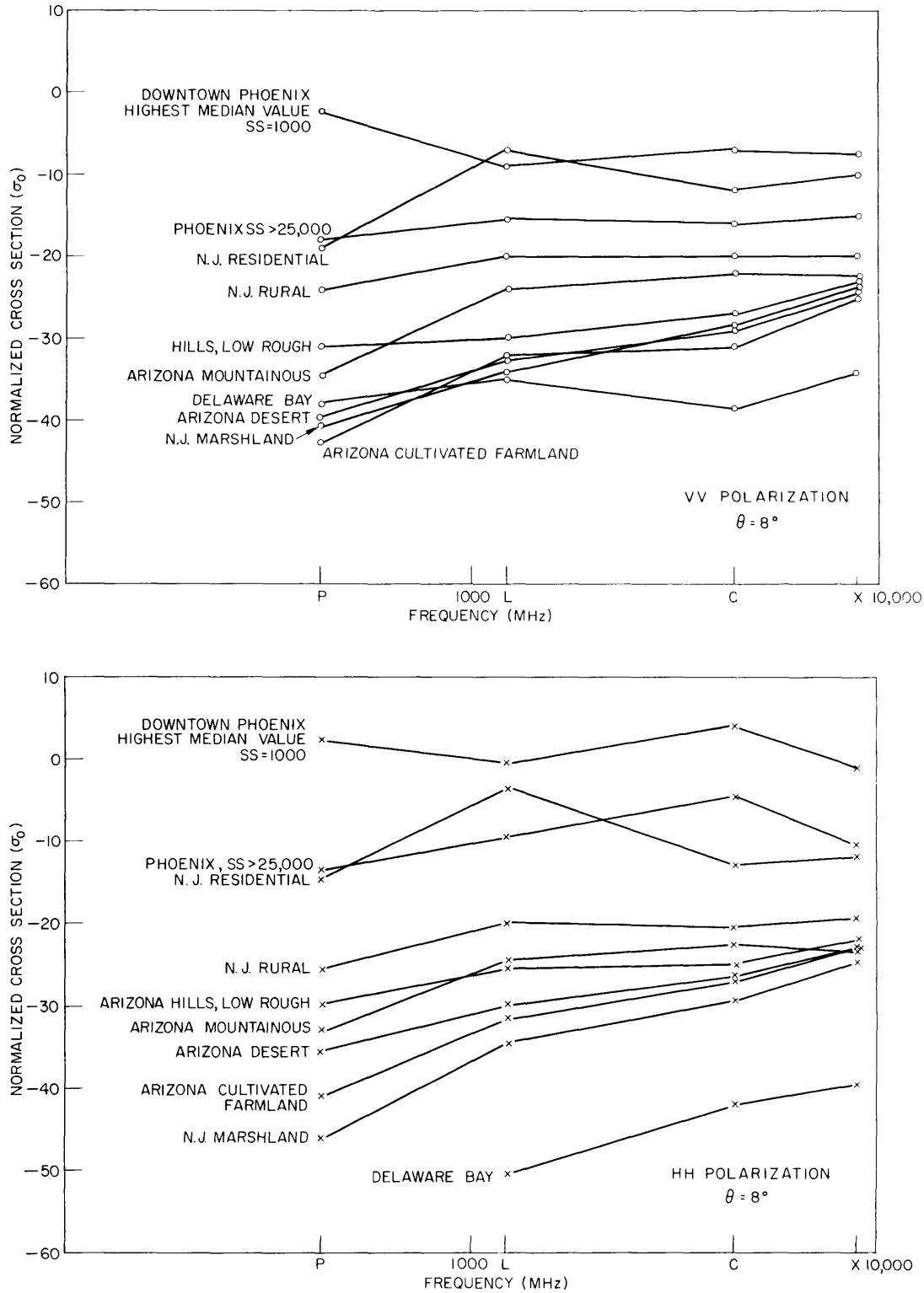

Fig. 16 - Normalized cross section vs wavelength

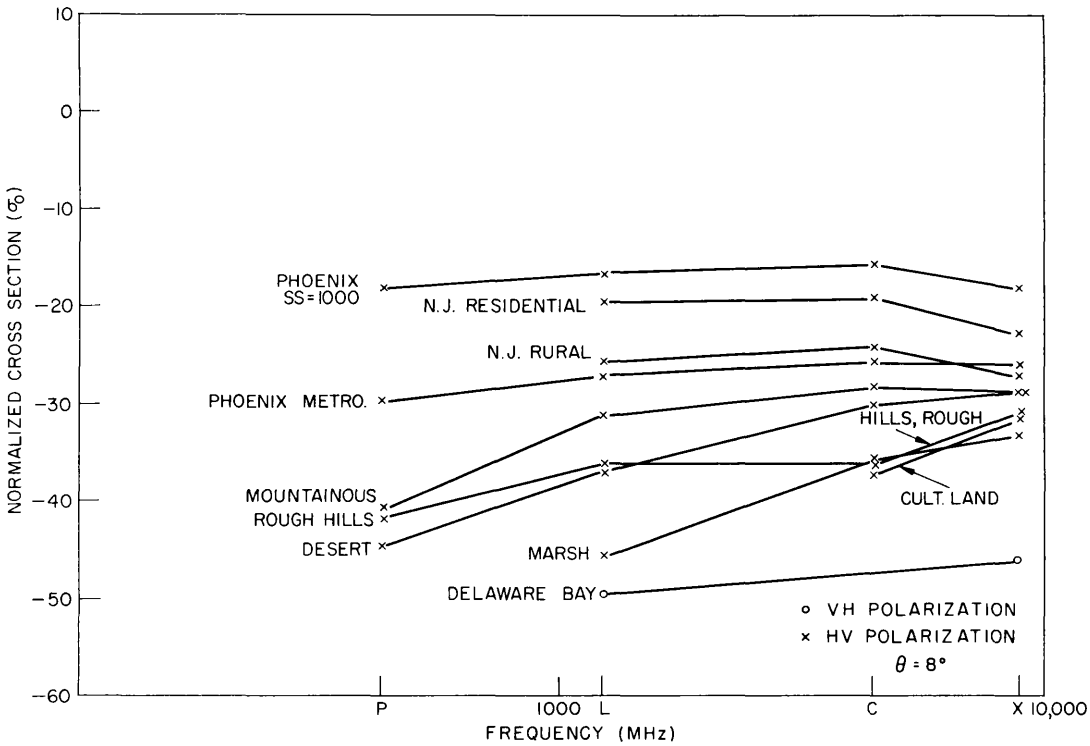

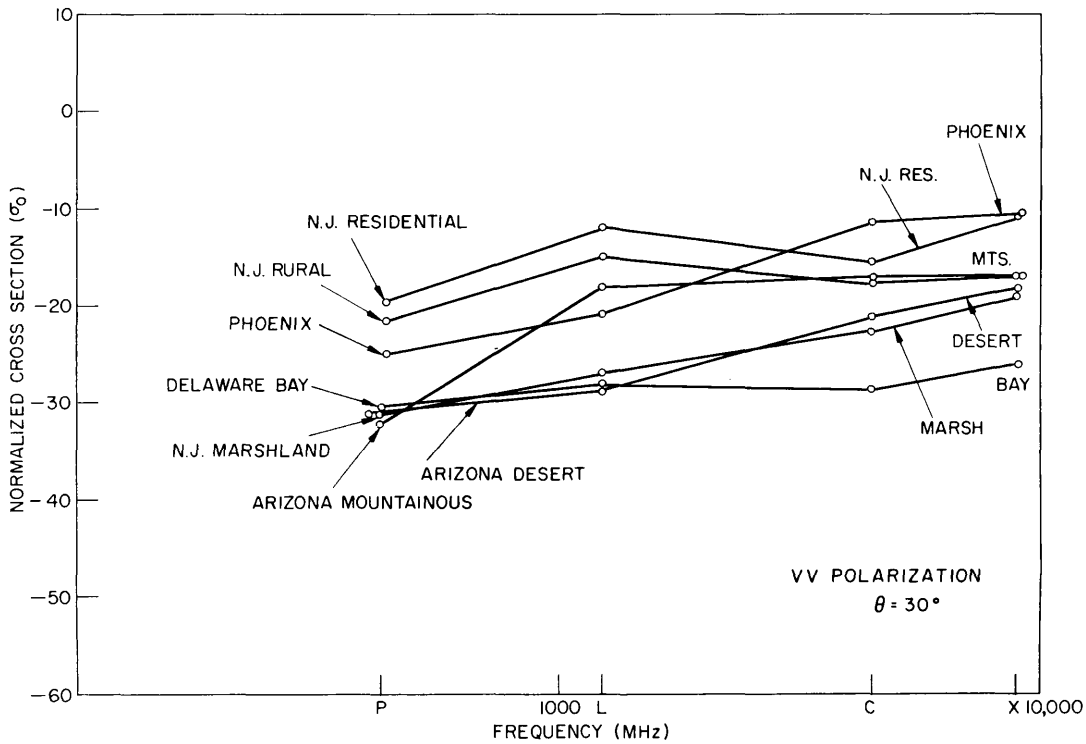

Fig. 16 (Continued) - Normalized cross section vs wavelength

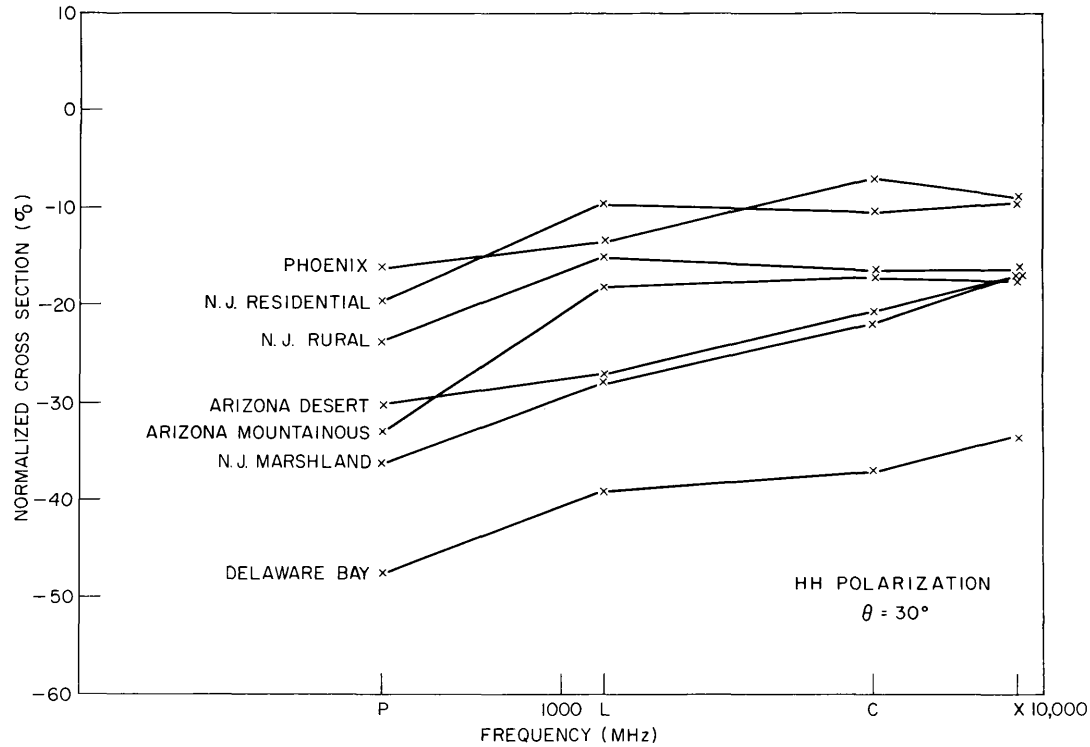

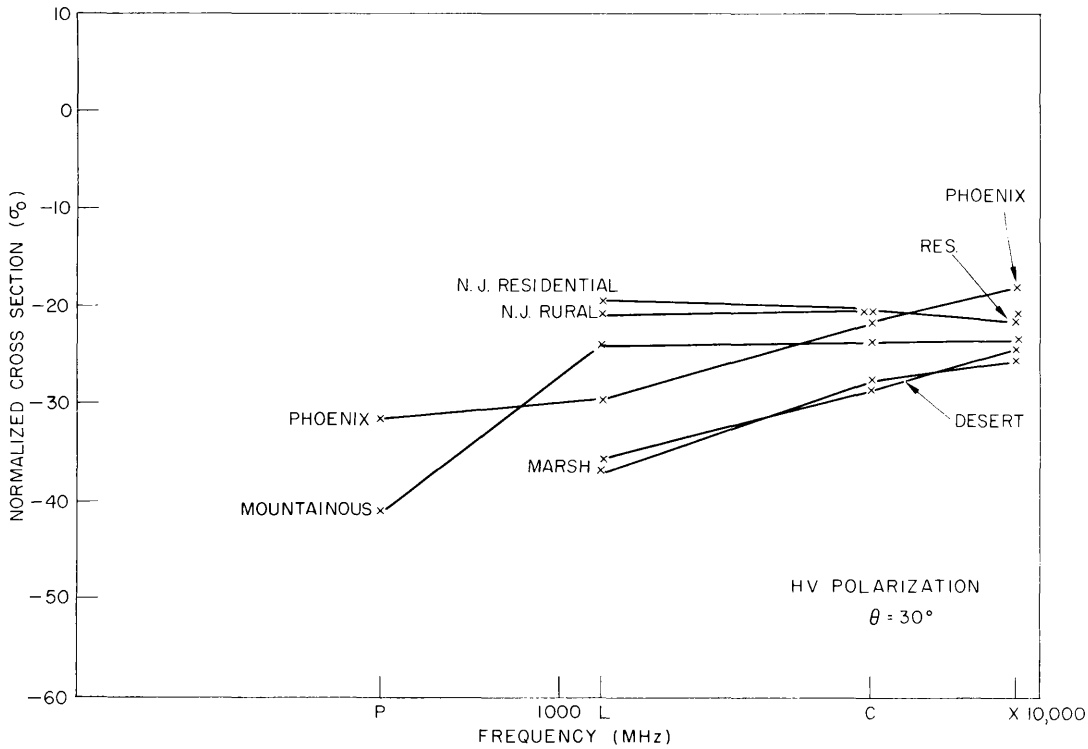

Fig. 16 (Continued) - Normalized cross section vs wavelength

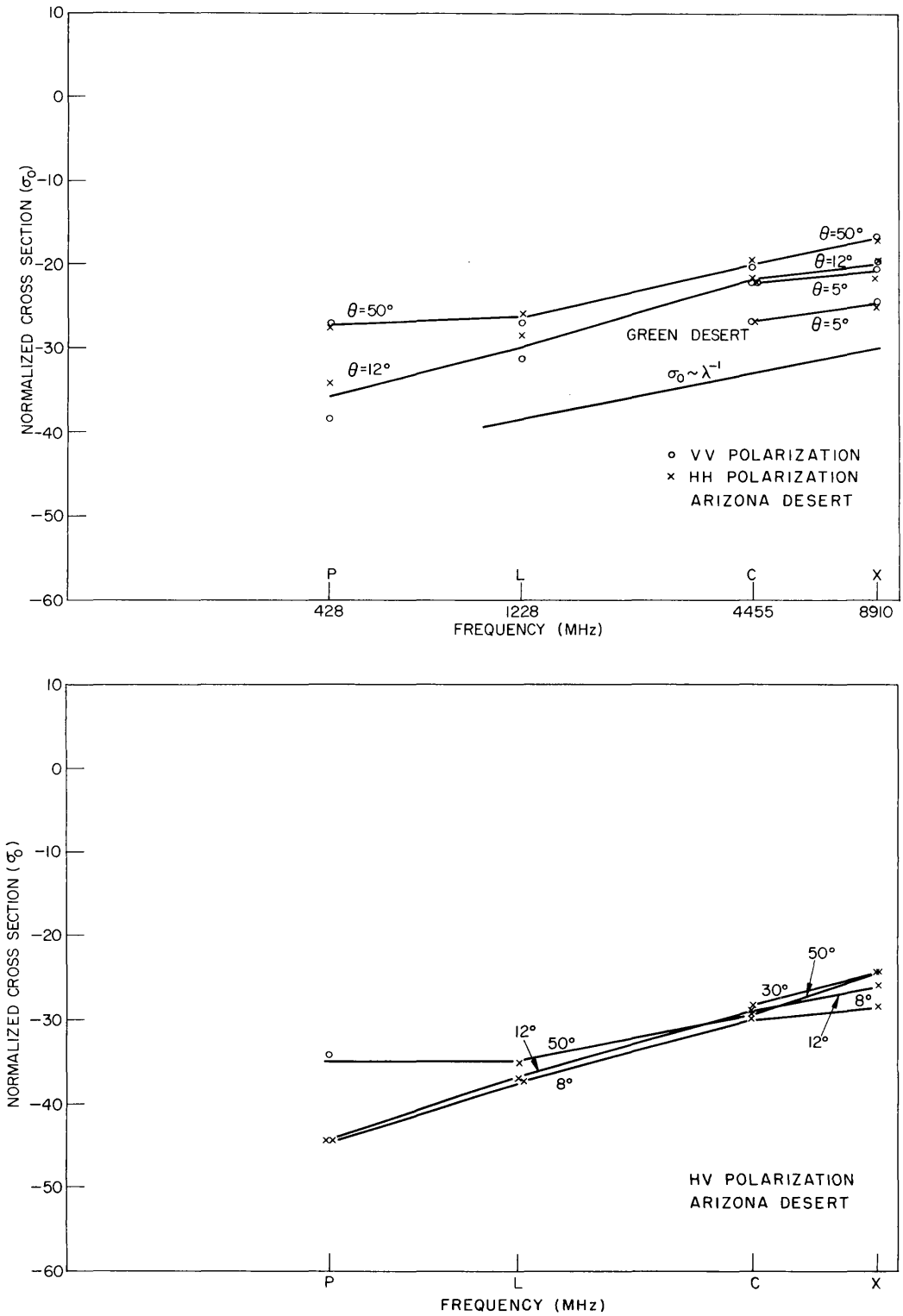

Fig. 17 - Wavelength dependence as a function of angle

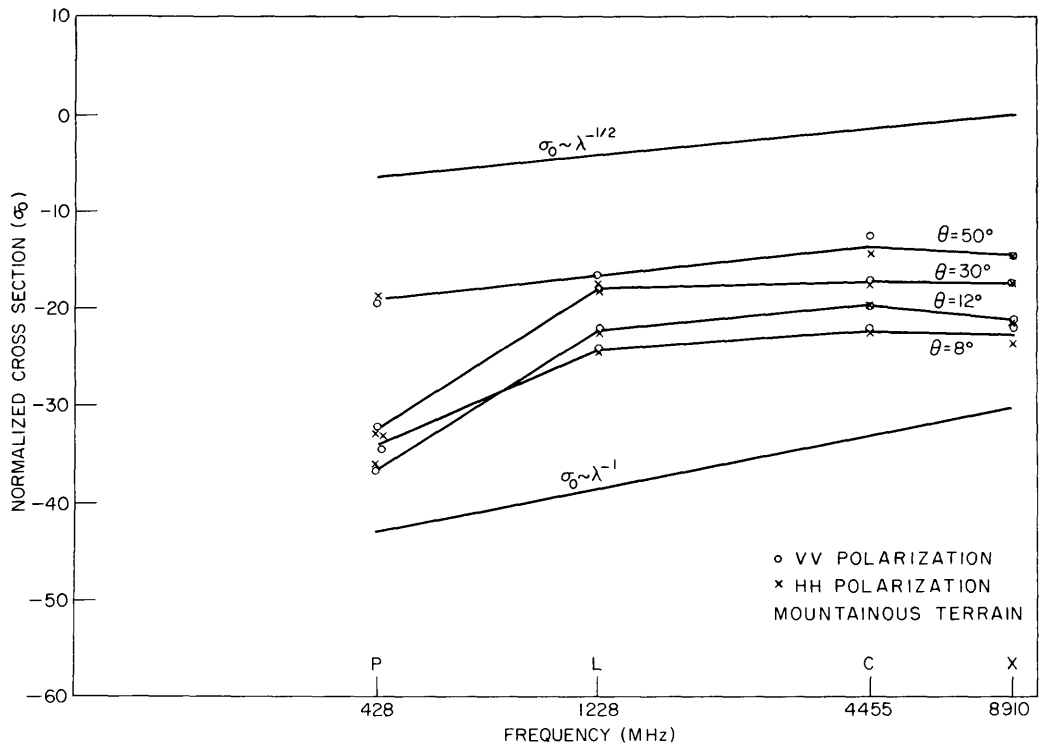

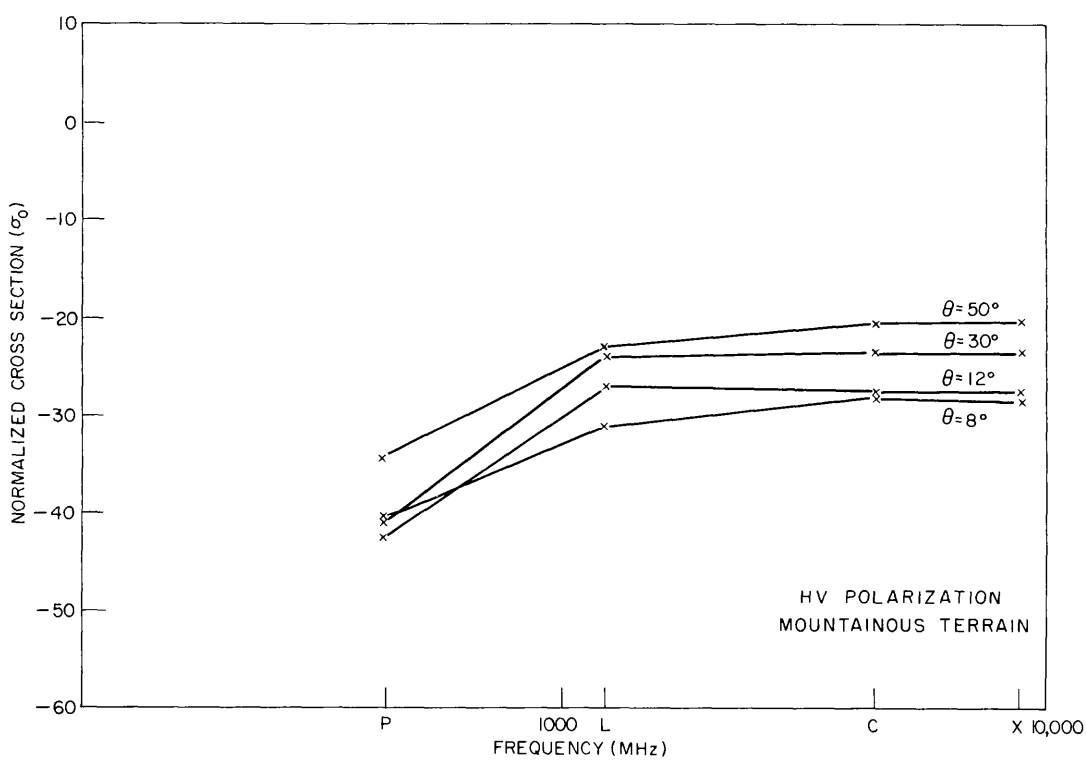

Fig. 17 (Continued) - Wavelength dependence as a function of angle

SYSTEMS LIMITATIONS

There are two basic sources of error in the absolute system calibrations as outlined (1): (a) receiver stability and (b) tracking error in the sphere measurement. The receiver stability is monitored, on a daily basis, by recording a known reference level at various time intervals. The variation of this reference level during the data recording and system calibration periods is given in Table 4 for each frequency and polarization.

Table 4
Receiver Stability on a Daily Basis

Frequency and Polarization	Stability (dB)			Sphere Tracking Error		
	10/6/66	10/7/66	1/30/66	10/6/66	10/7/66	1/30/67
X_V	±1	±1/4	±1/2	±1	±1-1/2	±1
X_H	±1/2	±1/4	±1/2	±1	±1	±1-1/4
C_V	±1	±1/2	±1-1/2	±1	±1-1/2	±1
C_H	±1/2	±1/2	±1/4	±1	±1-1/2	±1-1/4
L_V	±1/2	±1/2	±1/4	±1	±1	±1
L_H	±1/2	±1	0	±1	±1	±1
P_V	±1	±1/2	±1/2	±1-1/2	±2-1/2	±1-1/4
P_H	±1/2	±1/2	±1/2	±2	±3-1/2	±1-1/4

Also included in Table 4 are estimates of the accuracy of the sphere measurement. The error in the sphere measurement is chiefly caused by the variation of the position of the sphere within the antenna beam. This error is minimized by measuring several spheres for each calibration and using the strongest return at a given range. Previous data have shown that this procedure can reduce the tracking error to 2 dB or less. This estimate of the minimum tracking error is expressed as ±1 dB in Table 4. It is seen that greater limits are occasionally listed. This is true of cases where tracking the sphere was more difficult than usual and fewer runs were obtained.

Consequently, any given value of cross section is, within limits, specified by both factors of Table 4. However, a polarization ratio would contain only the stability error, since the tracking error is common. Wavelength ratios of X to C or L to P would likewise have, principally, stability errors, since the sphere is simultaneously illuminated by these frequencies.

In addition to the above factors, the measurement of cross-polarization cross sections involve such sources of error as antenna isolation and receiver crosstalk. The total system isolation for each frequency was estimated for each day, and contaminated cross-polarization components were eliminated. The cross-polarized data reported above are deemed free of crosstalk errors and subject only to the factors of receiver stability and sphere tracking discussed previously.

CONCLUSIONS

The second phase of the NRL clutter study has concentrated on the collection of terrain clutter data, first, for the implementation of a specific clutter model and second, to determine further information concerning the behavior of the normalized cross section

in the large scale. Measurements have been made over terrains which were selected to be homogeneous; namely, rural (New Jersey), marsh (New Jersey), Delaware Bay, desert, mountainous terrain, eroded desert, rough hills, and cultivated farmland. Data were also collected over nonhomogeneous terrain such as Phoenix and the Wildwood, New Jersey area. The data have been processed to yield both the statistics of small resolution cells measured parallel to the flight path and the statistics of large samples of terrain clutter.

This report has primarily concentrated on the large-scale variations in the normalized cross section of terrain. Table 5 summarizes the scattering characteristics of seven of the major terrain types in decreasing order of cross section for direct horizontal received polarization. In general, these may be summarized as follows:

(a) the normalized RCS is a slowly increasing function of the angle of incidence for most terrains with the exception of residential areas,

(b) the direct polarization ratio is largest for the Delaware Bay and marsh areas for L-band and P-band data and smallest over Phoenix urban terrain,

(c) the cross-polarization ratio is a maximum for urban and residential terrains,

(d) the wavelength dependence of the terrain clutter varies from $n \approx 0$ for urban terrain to $n \approx 3/2$ for marsh,

(e) the wavelength dependence is not a function of polarization or angle of incidence.

Table 5
Terrain Clutter, Summary

Terrain type	σ_0 (db); $\theta = 8°$				σ_0 vs Angle	σ_0 (VV)/σ_0 (HH)	σ_0(VV)/ σ_0(HV)	$\sigma_0 \propto \lambda^n$
	X_{HH} (max)	C_{HH} (max)	L_{HH} (max)	P_{HH} (max)				
Phoenix	- 1	+ 4	- 1/2	+ 2-1/2	Peaks at 8°	H> V	HV → +15	$\sigma_0 \propto \lambda^0$
New Jersey Residential	-12	-13	- 3-1/2	-14-1/2	Peaks at 8 to 15°		+8 → +10	
New Jersey Rural	-19-1/2	-20-1/2	-20	-25-1/2	Slowly increasing $\sigma_0 \propto \sin\theta$	H≧ V	+5 → +9	$\sigma_0 \propto \lambda^0$
Mountains	-23-1/2	-22-1/2	-24-1/2	-33				
Desert	-21	-22	-30	-35-1/2				$\sigma_0 \propto \lambda^{-1}$
Marsh	-24-1/2	-29-1/2	-34-1/2	-46	Strongly increasing			$\sigma_0 \propto \lambda^{-3/2}$
Delaware Bay	-39-1/2	-42	-50-1/2	<-53		V> H	None	No conclusion

REFERENCES

1. Guinard, N.W., Ransone, J.T., Jr., Laing, M.B., and Hearton, L.E., "NRL Terrain Clutter Study Phase I," NRL Report 6487, May 10, 1967

2. Greenstein, L.J., "Preliminary Design of a Clutter Model for Use in the Analysis of Overland Radar Systems," IIT Research Institute, Chicago, Illinois, unpublished note, Apr. 1966

3. Guinard, N.W., NRL letter 5270-2:NWG:bjg to IITRI, Chicago, Ill., of Jan. 24, 1967
   Guinard, N.W., NRL letter 5270-6:NWG:bjg to IITRI, Chicago, Ill., of Mar. 7, 1967
   Guinard, N.W., NRL letter 5270-16:NWG:bjg to IITRI, Chicago, Ill., of May 22, 1967
   Diggs, J.F., NRL letter 5270-30:JFD:bjg to IITRI, Chicago, Ill., of Nov. 8, 1967

4. Greenstein, L.J., Pipkin, R.F., Calhoun, L.C., "ORT Clutter Model - March 1968," Contract F33615-67-C-1387, of Mar. 22, 1968

5. Cosgriff, R.L., Peak, W.H., Taylor, R.C., The Antenna Laboratory, 29 (3), The Ohio State University, Columbus, May 1960

Appendix A

SAMPLE CLUTTER MAP

A clutter map for two frequencies, desert terrain, and incident angle of 12° consists of Tables A1 through A8. The tabular values are the selected percentile values of the cumulative probability distribution calculated on an arbitrary dB scale. These values may be converted to the absolute σ_0 scale by the addition of an appropriate constant. This constant is determined by the sphere measurement as described previously and is given for each signal component in Table A9.

It should be noted that median values of σ_0 obtained from the clutter maps will be slightly higher than those obtained by NRL from the 1000-pulse sample medians. This is due to averaging N pulses before the distribution step in processing the clutter map.

Table A1

DATE 10/06/66 RUN 110 FREQ X TPØL H RPØL V
CUMULATIVE PRØBABILITY DISTRIBUTIØNS
PERCENTILES IN DB
N= 3 K= 969
PARITY ERRØRS 0

	0	10	20	30	40	50	60	70	80	90
1	-30.7	-31.1	-31.3	-31.3	-31.4	-31.5	-31.5	-31.6	-31.6	-31.8
2	-30.7	-31.1	-31.3	-31.3	-31.5	-31.5	-31.5	-31.6	-31.6	-31.8
3	-23.2	-29.2	-31.0	-31.3	-31.5	-31.6	-31.8	-33.0	-37.6	-57.2
4	-3.0	-27.2	-28.2	-29.0	-29.5	-30.5	-31.4	-32.3	-33.4	-35.0
5	-14.8	-27.8	-28.7	-29.4	-30.2	-30.9	-31.9	-33.0	-34.0	-35.4
6	-4.7	-27.5	-28.6	-29.3	-30.0	-30.7	-31.5	-32.6	-33.6	-35.1
7	-19.1	-28.4	-29.4	-30.3	-31.0	-31.8	-32.7	-33.7	-34.8	-36.4
8	-7.1	-28.0	-29.2	-30.3	-31.1	-32.0	-33.0	-34.0	-35.0	-36.3
9	-7.6	-28.5	-29.6	-30.5	-31.3	-32.3	-33.2	-34.1	-35.0	-36.5
10	-9.8	-27.8	-29.0	-29.7	-30.5	-31.4	-32.3	-33.3	-34.2	-36.0
11	-2.6	-27.2	-28.3	-29.1	-29.9	-31.0	-31.9	-32.8	-33.9	-35.5
12	-24.2	-27.4	-28.3	-29.3	-30.0	-31.0	-31.7	-32.7	-33.8	-35.6
13	-5.5	-28.0	-29.2	-29.9	-31.0	-31.7	-32.8	-33.8	-35.1	-36.8
14	-8.1	-28.0	-29.2	-30.0	-30.9	-31.7	-32.5	-33.4	-34.6	-36.0
15	-5.7	-28.1	-29.1	-29.8	-30.7	-31.5	-32.4	-33.5	-34.5	-36.2
16	-2.5	-27.6	-28.5	-29.3	-30.1	-30.8	-31.7	-32.6	-33.9	-35.4
17	-24.0	-27.5	-28.6	-29.2	-29.8	-30.7	-31.5	-32.6	-33.8	-35.3
18	-4.2	-28.5	-29.5	-30.3	-31.2	-31.9	-32.9	-33.8	-35.0	-36.4
19	-25.9	-29.4	-30.4	-31.4	-32.3	-33.1	-34.0	-34.7	-35.6	-37.0
20	-25.4	-29.7	-31.0	-31.9	-33.0	-33.7	-34.5	-35.5	-36.5	-37.7

Table A2

DATE 10/06/66 RUN 110 FREQ X TPØL H RPØL H
CUMULATIVE PRØBABILITY DISTRIBUTIØNS
PERCENTILES IN DB
N= 3 K= 969
PARITY ERRØRS 0

	0	10	20	30	40	50	60	70	80	90
1	-18.4	-28.8	-28.9	-28.9	-29.0	-29.1	-29.2	-29.3	-29.3	-29.4
2	-17.7	-28.6	-28.8	-28.9	-29.0	-29.1	-29.2	-29.3	-29.3	-29.4
3	-14.7	-19.4	-21.5	-23.9	-28.6	-28.9	-29.1	-29.3	-29.7	-55.0
4	-12.8	-17.5	-18.4	-19.4	-20.2	-20.8	-21.5	-22.2	-23.2	-24.6
5	-13.6	-17.6	-18.6	-19.5	-20.3	-21.1	-21.9	-22.7	-23.7	-25.0
6	-13.7	-17.9	-19.1	-19.9	-20.8	-21.6	-22.4	-23.2	-24.3	-25.8
7	-14.0	-18.6	-19.8	-20.5	-21.2	-22.1	-22.9	-23.6	-24.7	-26.3
8	-15.2	-18.7	-19.8	-20.6	-21.4	-22.1	-22.9	-23.8	-24.9	-26.7
9	-13.4	-18.3	-19.3	-20.3	-21.1	-21.8	-22.6	-23.4	-24.5	-26.2
10	-13.4	-17.9	-19.1	-20.0	-20.8	-21.4	-22.1	-23.0	-24.1	-25.5
11	-10.9	-17.9	-19.0	-19.9	-20.6	-21.3	-22.1	-22.9	-23.9	-25.9
12	-13.9	-17.7	-18.9	-19.6	-20.4	-21.1	-21.9	-22.7	-23.6	-25.0
13	-11.6	-18.2	-19.3	-20.0	-20.7	-21.6	-22.4	-23.2	-24.3	-25.9
14	-12.2	-18.1	-19.2	-20.0	-20.7	-21.5	-22.3	-23.2	-24.2	-25.7
15	-9.4	-18.3	-19.3	-20.2	-21.0	-21.8	-22.6	-23.4	-24.4	-25.9
16	-12.1	-18.2	-19.3	-20.0	-20.8	-21.5	-22.3	-23.2	-24.1	-25.8
17	-13.0	-17.7	-19.0	-19.8	-20.4	-21.1	-21.9	-22.7	-23.6	-25.0
18	-14.9	-18.8	-19.9	-20.6	-21.3	-22.1	-22.9	-23.9	-24.9	-26.7
19	-16.3	-19.4	-20.4	-21.2	-21.9	-22.5	-23.2	-23.9	-24.8	-26.4
20	-7.6	-19.3	-20.7	-21.6	-22.3	-23.0	-23.7	-24.6	-25.7	-27.3

Table A3

DATE 10/06/66 RUN 110 FREQ X TPØL V RPØL V
CUMULATIVE PRØBABILITY DISTRIBUTIØNS
PERCENTILES IN DB
N= 3 K= 969
PARITY ERRØRS 0

	0	10	20	30	40	50	60	70	80	90
1	-31.3	-31.6	-31.8	-31.8	-31.8	-31.8	-32.0	-32.0	-32.1	-32.1
2	-30.4	-31.6	-31.6	-31.8	-31.8	-31.8	-32.0	-32.0	-32.1	-32.1
3	-6.6	-23.1	-24.7	-27.1	-31.6	-31.8	-31.8	-32.0	-32.6	-56.9
4	-5.5	-20.9	-22.0	-23.0	-23.6	-24.5	-25.3	-26.0	-26.9	-27.1
5	-16.7	-21.7	-22.8	-23.6	-24.3	-25.0	-25.6	-26.5	-27.4	-28.8
6	-16.2	-21.5	-22.7	-23.6	-24.2	-25.1	-25.8	-26.6	-27.4	-27.8
7	-16.7	-22.7	-23.8	-24.6	-25.4	-25.9	-26.7	-27.5	-28.4	-29.5
8	-2.3	-22.9	-23.9	-24.8	-25.5	-26.3	-26.9	-27.6	-28.7	-30.1
9	-4.3	-23.4	-24.5	-25.3	-26.1	-26.7	-27.2	-27.9	-28.9	-30.1
10	-10.4	-22.7	-24.1	-24.9	-25.6	-26.3	-27.0	-27.6	-28.6	-29.8
11	-17.6	-22.6	-23.6	-24.4	-25.2	-25.9	-26.6	-27.4	-28.3	-29.7
12	-17.6	-22.0	-23.2	-24.1	-24.8	-25.5	-26.2	-26.9	-27.8	-29.0
13	-4.7	-23.0	-24.4	-25.3	-25.9	-26.7	-27.2	-28.1	-29.1	-30.4
14	-4.7	-23.1	-24.2	-24.9	-25.6	-26.2	-26.9	-27.6	-28.5	-29.7
15	-6.0	-22.4	-23.6	-24.5	-25.3	-25.9	-26.5	-27.2	-28.2	-29.4
16	-1.0	-21.9	-23.0	-23.9	-24.5	-25.3	-25.9	-26.6	-27.2	-28.4
17	-18.2	-22.0	-22.9	-23.8	-24.5	-25.4	-26.0	-26.7	-27.5	-28.9
18	-3.3	-23.0	-24.1	-24.8	-25.5	-26.2	-26.9	-27.6	-28.6	-29.9
19	-18.8	-23.8	-24.9	-25.6	-26.3	-26.9	-27.4	-28.2	-29.1	-30.5
20	-4.6	-24.2	-25.2	-25.9	-26.6	-27.1	-27.9	-28.5	-29.5	-31.2

Table A4

DATE 10/06/66 RUN 110 FREQ X TPØL V RPØL H
CUMULATIVE PRØBABILITY DISTRIBUTIØNS
PERCENTILES IN DB
N= 3 K= 969
PARITY ERRØRS 0

	0	10	20	30	40	50	60	70	80	90
1	-19.1	-28.3	-28.4	-28.6	-28.6	-28.8	-28.9	-28.9	-29.0	-29.2
2	-16.8	-28.3	-28.4	-28.6	-28.6	-28.8	-28.9	-28.9	-29.0	-29.2
3	-13.7	-25.2	-27.3	-28.2	-28.4	-28.7	-28.9	-29.2	-33.1	-55.2
4	-11.5	-23.3	-24.4	-25.2	-26.0	-26.7	-27.5	-28.3	-29.0	-30.3
5	-18.0	-23.6	-24.7	-25.6	-26.4	-27.0	-27.9	-28.7	-29.5	-30.9
6	-17.1	-23.4	-24.5	-25.4	-26.1	-26.6	-27.3	-28.1	-29.1	-30.4
7	-20.4	-24.5	-25.6	-26.5	-27.2	-27.8	-28.4	-29.1	-30.1	-31.9
8	-12.1	-24.4	-25.5	-26.4	-27.1	-27.7	-28.5	-29.3	-30.1	-31.9
9	-8.9	-24.4	-25.5	-26.4	-27.0	-27.7	-28.4	-29.2	-30.0	-31.4
10	-14.4	-23.9	-25.1	-25.9	-26.6	-27.3	-27.9	-28.7	-29.7	-31.0
11	-7.5	-23.0	-24.4	-25.2	-26.0	-26.7	-27.3	-28.2	-29.2	-31.1
12	-19.7	-23.2	-24.5	-25.3	-26.1	-26.7	-27.4	-28.1	-29.0	-30.3
13	-14.2	-24.1	-25.2	-26.1	-26.9	-27.4	-28.2	-28.9	-30.1	-31.5
14	-13.3	-24.0	-25.3	-26.2	-26.9	-27.6	-28.3	-29.0	-29.9	-31.1
15	-7.3	-24.1	-25.2	-26.1	-26.7	-27.4	-28.1	-28.8	-29.7	-31.1
16	-19.1	-23.6	-24.5	-25.4	-26.1	-26.9	-27.7	-28.3	-29.4	-30.7
17	-19.9	-23.3	-24.4	-25.3	-26.0	-26.8	-27.5	-28.2	-29.0	-30.2
18	-8.5	-24.4	-25.6	-26.4	-27.2	-27.8	-28.6	-29.4	-30.2	-31.5
19	-21.4	-25.6	-26.5	-27.3	-28.0	-28.6	-29.3	-30.0	-30.7	-32.6
20	-13.6	-25.9	-27.0	-27.8	-28.5	-29.1	-29.7	-30.5	-31.5	-32.9

Table A5

DATE 10/06/66 RUN 110 FREQ C TPØL H RPØL V
CUMULATIVE PRØBABILITY DISTRIBUTIØNS
PERCENTILES IN DB
N= 6 K= 517
PARITY ERRØRS 0

	0	10	20	30	40	50	60	70	80	90
1	-16.7	-36.3	-36.4	-36.4	-36.5	-36.5	-36.5	-36.5	-36.6	-36.7
2	-17.4	-36.3	-36.3	-36.4	-36.4	-36.4	-36.5	-36.5	-36.5	-36.6
3	-7.3	-30.0	-31.8	-33.3	-34.8	-36.3	-36.5	-36.5	-37.9	-53.0
4	-6.2	-29.2	-30.5	-31.3	-32.2	-32.9	-33.5	-34.4	-35.3	-36.4
5	-8.2	-29.2	-30.5	-31.3	-32.1	-32.8	-33.6	-34.3	-35.1	-36.4
6	-26.1	-29.1	-30.3	-31.1	-31.8	-32.6	-33.2	-34.1	-35.0	-36.2
7	-6.5	-29.7	-31.1	-32.1	-32.8	-33.4	-34.2	-34.7	-35.7	-36.8
8	-5.0	-30.3	-31.5	-32.5	-33.2	-34.0	-34.6	-35.2	-35.9	-36.9
9	-25.4	-29.7	-30.7	-31.7	-32.4	-33.1	-33.9	-34.5	-35.3	-36.2
10	-5.6	-29.4	-30.7	-31.8	-32.7	-33.4	-34.0	-34.7	-35.5	-36.4
11	-10.9	-29.7	-31.0	-32.0	-32.7	-33.5	-34.2	-34.8	-35.7	-37.0
12	-25.9	-30.5	-31.6	-32.6	-33.3	-34.0	-34.6	-35.1	-36.0	-37.1
13	-6.0	-29.8	-31.4	-32.4	-33.2	-34.0	-34.5	-35.2	-36.1	-37.3
14	-5.5	-30.3	-31.4	-32.4	-33.2	-33.9	-34.5	-35.3	-36.0	-37.3
15	-4.9	-29.9	-31.0	-31.7	-32.5	-33.2	-33.9	-34.9	-35.6	-36.9
16	-9.0	-30.0	-31.1	-32.0	-32.8	-33.5	-34.3	-34.9	-35.5	-36.6
17	-6.5	-30.9	-32.3	-33.2	-33.7	-34.4	-35.0	-35.7	-36.5	-37.7
18	-26.4	-31.2	-32.3	-33.0	-33.7	-34.5	-35.2	-35.8	-36.8	-37.9
19	-19.3	-31.2	-32.7	-33.5	-34.2	-34.9	-35.5	-36.1	-37.0	-38.1

Table A6

DATE 10/06/66 RUN 110 FREQ C TPØL H RPØL H
CUMULATIVE PRØBABILITY DISTRIBUTIØNS
PERCENTILES IN DB
N= 6 K= 517
PARITY ERRØRS 0

	0	10	20	30	40	50	60	70	80	90
1	-17.0	-35.3	-35.3	-35.4	-35.5	-35.5	-35.6	-35.6	-35.7	-35.8
2	-18.0	-35.4	-35.5	-35.6	-35.6	-35.7	-35.7	-35.8	-35.9	-36.0
3	-16.1	-26.4	-27.6	-28.5	-29.8	-32.3	-35.5	-35.7	-35.9	-54.9
4	-7.5	-25.2	-26.2	-27.0	-27.6	-28.2	-28.8	-29.2	-30.1	-31.2
5	-7.3	-25.7	-26.6	-27.2	-27.8	-28.4	-28.9	-29.6	-30.4	-32.0
6	-21.4	-26.1	-26.9	-27.7	-28.3	-28.8	-29.5	-30.1	-30.9	-32.1
7	-13.1	-26.7	-27.8	-28.3	-29.0	-29.6	-30.3	-31.0	-31.7	-33.0
8	-9.3	-26.4	-27.5	-28.2	-28.8	-29.5	-30.1	-30.8	-31.8	-33.2
9	-22.2	-25.4	-26.6	-27.4	-28.1	-28.8	-29.4	-29.9	-30.8	-32.0
10	-9.6	-26.0	-27.2	-27.9	-28.6	-29.0	-29.7	-30.5	-31.4	-32.8
11	-23.8	-26.1	-27.3	-27.9	-28.6	-29.1	-29.8	-30.5	-31.4	-32.6
12	-21.4	-26.3	-27.4	-28.0	-28.6	-29.1	-29.8	-30.3	-31.1	-32.1
13	-10.5	-26.0	-27.3	-27.9	-28.4	-29.2	-29.8	-30.5	-31.1	-32.7
14	-22.3	-26.1	-27.1	-27.8	-28.4	-29.0	-29.7	-30.4	-31.4	-32.7
15	-13.6	-26.1	-27.2	-27.8	-28.4	-29.1	-29.8	-30.5	-31.2	-32.4
16	-16.4	-25.4	-26.7	-27.3	-27.9	-28.6	-29.1	-29.9	-30.8	-31.9
17	-22.7	-26.9	-28.0	-28.6	-29.2	-29.9	-30.5	-31.3	-32.2	-33.4
18	-24.2	-27.4	-28.3	-28.9	-29.5	-30.1	-30.9	-31.4	-32.3	-33.3
19	-8.1	-27.8	-28.9	-29.5	-30.1	-30.7	-31.3	-31.9	-33.1	-34.3

Table A7

DATE 10/06/66 RUN 110 FREQ C TPØL V RPØL V
CUMULATIVE PRØBABILITY DISTRIBUTIØNS
PERCENTILES IN DB
N= 6 K= 517
PARITY ERRØRS 0

	0	10	20	30	40	50	60	70	80	90
1	-16.8	-36.6	-36.7	-36.7	-36.7	-36.8	-36.8	-36.9	-36.9	-37.0
2	-17.2	-36.5	-36.6	-36.7	-36.7	-36.7	-36.8	-36.8	-36.9	-36.9
3	-10.0	-23.6	-24.9	-26.0	-27.4	-29.5	-36.6	-36.7	-36.9	-52.8
4	-7.4	-22.7	-23.7	-24.4	-25.1	-25.8	-26.4	-26.9	-27.6	-27.9
5	-7.5	-23.2	-24.3	-24.9	-25.6	-26.3	-26.9	-27.5	-28.3	-29.7
6	-18.6	-22.7	-23.8	-24.4	-25.1	-25.7	-26.3	-26.9	-27.7	-29.0
7	-7.3	-23.8	-24.8	-25.6	-26.2	-26.8	-27.4	-28.1	-29.1	-30.3
8	-6.0	-24.4	-25.4	-26.0	-26.7	-27.3	-28.0	-28.9	-29.4	-31.0
9	-19.5	-23.7	-24.8	-25.4	-26.2	-26.7	-27.3	-28.0	-28.9	-30.3
10	-6.6	-23.7	-24.9	-25.4	-26.3	-26.9	-27.5	-28.2	-29.4	-30.8
11	-20.5	-23.8	-24.7	-25.5	-26.0	-26.5	-27.1	-27.8	-28.6	-29.8
12	-21.6	-24.5	-25.5	-26.1	-26.7	-27.4	-28.2	-28.8	-29.6	-30.9
13	-8.6	-23.9	-25.2	-25.6	-26.5	-27.1	-27.9	-28.6	-29.5	-30.9
14	-11.2	-24.2	-25.2	-25.9	-26.5	-27.0	-27.6	-28.2	-29.0	-30.6
15	-10.0	-23.4	-24.2	-25.1	-25.7	-26.2	-26.8	-27.4	-28.3	-29.7
16	-7.4	-23.3	-24.3	-25.1	-25.8	-26.4	-27.0	-27.7	-28.3	-29.4
17	-19.5	-24.5	-25.6	-26.3	-26.7	-27.3	-27.9	-28.6	-29.5	-31.1
18	-21.0	-24.7	-25.8	-26.6	-27.2	-27.9	-28.6	-29.2	-30.2	-31.8
19	-5.5	-24.8	-25.9	-26.8	-27.3	-27.8	-28.4	-29.1	-30.2	-31.7

Table A8

DATE 10/06/66 RUN 110 FREQ C TPØL V RPØL H
CUMULATIVE PRØBABILITY DISTRIBUTIØNS
PERCENTILES IN DB
N= 6 K= 517
PARITY ERRØRS 0

	0	10	20	30	40	50	60	70	80	90
1	-17.1	-34.6	-34.7	-34.7	-34.8	-34.8	-34.9	-34.9	-34.9	-35.1
2	-17.0	-34.7	-34.8	-34.8	-34.9	-34.9	-35.0	-35.1	-35.1	-35.3
3	-7.1	-29.9	-31.1	-32.9	-34.4	-34.8	-34.9	-35.2	-37.8	-55.0
4	-16.8	-29.3	-30.2	-31.1	-31.6	-32.4	-33.2	-33.9	-34.6	-36.0
5	-10.0	-29.2	-30.2	-30.9	-31.6	-32.2	-33.0	-33.7	-34.7	-35.9
6	-25.9	-29.1	-29.9	-30.7	-31.4	-32.2	-32.8	-33.4	-34.5	-35.6
7	-8.6	-29.6	-30.6	-31.5	-32.2	-33.0	-33.7	-34.5	-35.4	-36.4
8	-8.7	-30.1	-31.0	-31.8	-32.5	-33.0	-33.9	-34.6	-35.3	-36.5
9	-25.1	-29.4	-30.2	-30.9	-31.5	-32.2	-33.0	-33.6	-34.6	-35.9
10	-13.8	-29.3	-30.5	-31.3	-32.0	-32.7	-33.3	-34.2	-34.9	-36.0
11	-16.1	-29.5	-30.4	-31.3	-32.0	-32.6	-33.2	-33.9	-34.8	-35.9
12	-26.9	-29.9	-31.0	-31.8	-32.4	-33.3	-33.7	-34.4	-35.2	-36.3
13	-12.5	-29.5	-30.7	-31.5	-32.3	-33.0	-33.6	-34.3	-35.3	-36.5
14	-7.2	-29.8	-30.9	-31.8	-32.5	-33.3	-34.0	-34.5	-35.2	-36.5
15	-9.9	-29.9	-30.8	-31.5	-32.3	-32.8	-33.4	-34.1	-34.9	-36.1
16	-9.0	-29.6	-30.6	-31.5	-32.1	-32.7	-33.4	-33.9	-34.7	-36.1
17	-5.6	-30.5	-31.7	-32.5	-33.2	-33.8	-34.5	-35.0	-35.9	-37.1
18	-26.4	-30.4	-31.6	-32.3	-33.0	-33.7	-34.5	-35.1	-36.1	-37.3
19	-26.5	-30.7	-32.2	-32.7	-33.5	-34.2	-34.9	-35.8	-36.6	-37.6

Table A9

Additive Constant for Run 110 (in dB)

X_{VV}	X_{HV}	X_{HH}	X_{VH}	C_{VV}	C_{HV}	C_{HH}	C_{VH}
+16	+16	+12-1/2	+12-1/2	+15	+15	+17-1/2	+17-1/2

Security Classification

DOCUMENT CONTROL DATA - R & D

(Security classification of title, body of abstract and indexing annotation must be entered when the overall report is classified)

1. ORIGINATING ACTIVITY *(Corporate author)* Naval Research Laboratory Washington, D.C., 20390	2a. REPORT SECURITY CLASSIFICATION Unclassified 2b. GROUP

3. REPORT TITLE

NRL TERRAIN CLUTTER STUDY PHASE II

4. DESCRIPTIVE NOTES *(Type of report and inclusive dates)*

This is a final report on the problem.

5. AUTHOR(S) *(First name, middle initial, last name)*

John C. Daley, Willie T. Davis, James R. Duncan, Michael B. Laing

6. REPORT DATE	7a. TOTAL NO. OF PAGES	7b. NO. OF REFS
October 21, 1968	44	5

8a. CONTRACT OR GRANT NO. NRL Problem R07-02 b. PROJECT NO. AF MIPR AS-6-157 c. d.	9a. ORIGINATOR'S REPORT NUMBER(S) NRL Report 6749 9b. OTHER REPORT NO(S) *(Any other numbers that may be assigned this report)*

10. DISTRIBUTION STATEMENT

This document has been approved for public release and sale; its distribution is unlimited.

11. SUPPLEMENTARY NOTES	12. SPONSORING MILITARY ACTIVITY Department of the Air Force (Wright-Patterson AFB, Ohio)

13. ABSTRACT

The second and final phase of a terrain clutter study has been completed at Naval Research Laboratory utilizing the Four-Frequency Radar System installed in a WV-2 (Super Constellation) aircraft, BuNo 128324. This system is capable of transmitting and receiving four frequencies (P,X,L, and C) consecutively with a choice of horizontal, vertical, and alternating polarizations. The returns are gated at a fixed range and analyzed in a digital computer. Absolute clutter measurements have been taken over several sites at angles of incidence from 5 degrees to 60 degrees. The parameter measured was the normalized radar cross section in terms of the median value of its probability distribution. Data were obtained for this parameter as a function of incident angle, transmitted and received polarization, and radar wavelength for a wide variety of terrain types such as desert, mountainous, urban, and water. A significant conclusion was that the wavelength dependence of the terrain clutter varies from $n \approx 0$ for urban terrain to $n \approx 3/2$ for marshes.

DD FORM 1 NOV 65 1473 (PAGE 1)

S/N 0101-807-6801

Security Classification

14. KEY WORDS	LINK A ROLE	LINK A WT	LINK B ROLE	LINK B WT	LINK C ROLE	LINK C WT
Radar						
Research						
Terrain clutter						
Surface effects						
Scatter						
Backscatter						
Normalized cross-section data						
Four-frequency radar system						
X, C, L, and P frequency data						

DD FORM 1 NOV 65 1473 (BACK)
(PAGE 2)